Mapping and Monitoring of Vegetation using Airborne Laser Scanning

Mattias Nyström
Faculty of Forest Sciences
Department of Forest Resource Management
Umeå

Doctoral Thesis
Swedish University of Agricultural Sciences
Umeå 2014

Acta Universitatis agriculturae Sueciae
2014:9

Cover: View from sample plot 1089 in Abisko, June 24, 2010.
(photo: Mattias Nyström)

ISSN 1652-6880
ISBN (print version) 978-91-576-7966-6
ISBN (electronic version) 978-91-576-7967-3

Print: Arkitektkopia, Umeå 2014

Mapping and monitoring of vegetation using airborne laser scanning

Abstract

In this thesis, the utility of airborne laser scanning (ALS) for monitoring vegetation of relevance for the environmental sector was investigated. The vegetation characteristics studied include measurements of biomass, biomass change and vegetation classification in the forest-tundra ecotone; afforestation of grasslands; and detection of windthrown trees. Prediction of tree biomass for mountain birch (*Betula pubescens* ssp. *czerepanovii*) using sparse (1.4 points/m^2) and dense (6.1 points/m^2) ALS data was compared for a site at the forest-tundra ecotone near Abisko in northern Sweden (Lat. 68° N, Long. 19° E). The predictions using the sparse ALS data provided almost as good results (RMSE 21.2%) as the results from the dense ALS data (18.7%) despite the large difference in point densities. A new algorithm was developed to compensate for uneven distribution of the laser points without decimating the data; use of this algorithm reduced the RMSE for biomass prediction from 19.9% to 18.7% for the dense ALS data. Additional information about vegetation height and density from ALS data improved a satellite data classification of alpine vegetation, in particular for the willow and mountain birch classes. Histogram matching was shown to be effective for relative calibration of metrics from two ALS acquisitions collected over the same area using different scanners and flight parameters. Thus the difference between histogram-matched ALS metrics from different data acquisitions can be used to locate areas with unusual development of the vegetation.

The height of small trees (0.3–2.6 m tall) in former pasture land near the Remningstorp test site in southern Sweden (Lat. 58° N, Long. 13° E) could be measured with high precision (standard deviation 0.3 m) using high point density ALS data (54 points/m^2). When classifying trees taller than 1 m into the two classes of changed and unchanged, the overall classification accuracy was 88%. A new method to automatically detect windthrown trees in forested areas was developed and evaluated at the Remningstorp test site. The overall detection rate was 38% on tree-level, but when aggregating to 40 m square grid cells, at least one windthrown tree was detected in 77% of the cells that according to field data contained windthrown trees.

In summary, this thesis has shown the high potential for ALS to be a future tool to map and monitor vegetation for several applications of interest for the environmental sector.

Keywords: airborne laser scanning; ALS; LiDAR; biomass; mountain birch; alpine vegetation; change detection; afforestation; windthrown trees

Author's address: Mattias Nyström, SLU, Department of Forest Resource Management, Skogsmarksgränd 1, 901 83 Umeå, Sweden. *E-mail:* mattias.nystrom@slu.se

If I were creating the world, I wouldn't mess about with butterflies and daffodils. I would have started with lasers, eight o'clock, Day One!

Time Bandits

Contents

List of Publications

This thesis is based on the work contained in the following papers, referred to by Roman numerals in the text:

I Nyström, M., Holmgren, J., & Olsson, H. (2012). Prediction of tree biomass in the forest–tundra ecotone using airborne laser scanning. *Remote Sensing of Environment* 123, 271-279.

II Reese, H., Nyström, M., Nordkvist, K., & Olsson, H. (2014). Combining airborne laser scanning data and optical satellite data for classification of alpine vegetation. *International Journal of Applied Earth Observation and Geoinformation* 27, 81-90.

III Nyström, M., Holmgren, J., & Olsson, H. (2013). Change detection of mountain birch using multi-temporal ALS point clouds. *Remote Sensing Letters* 4, 190-199.

IV Nyström, M., Holmgren, J., & Olsson, H. (2013). Detecting afforestation at individual tree level using ALS (manuscript).

V Nyström, M., Holmgren, J., Fransson, J. E. S., & Olsson, H. Detection of windthrown trees using airborne laser scanning. Accepted for publication in *International Journal of Applied Earth Observation and Geoinformation*.

The contribution of Mattias Nyström to the papers included in this thesis was as follows:

I Planned the field inventory in co-operation with the supervisors. Carried out the field data collection, developed the models, performed the analysis, and wrote the major part of the manuscript.

II Developed and calculated the laser metrics used in the classification.

III Planned the field inventory in co-operation with the supervisors. Carried out the field work, developed the methods, performed the analysis, and wrote the major part of the manuscript.

IV Planned the field inventory in co-operation with the supervisors. Carried out the field work, developed the methods except for the active surface algorithm, performed the analysis, and wrote the major part of the manuscript.

V Developed most of the methods except for the active surface algorithm, performed the analysis, and wrote the major part of the manuscript.

Abbreviations

3D	Three-dimensional
a.g.l.	Above ground level
AGB	Above ground biomass
ALS	Airborne laser scanning
CH	Canopy height
CHM	Canopy height model
DBH	Diameter at breast height
DEM	Digital elevation model
DGPS	Differential GPS
DSM	Digital surface model
GNSS	Global Navigation Satellite Systems
GPS	Global Positioning System
HRG	High resolution geometrical (SPOT 5 HRG = 10 m pixels)
LAI	Leaf area index
LAS	LASer file format
LDA	Linear discriminant analysis
LiDAR	Light detection and ranging
MH	Maximum height
nDSM	Normalized digital surface model
NDII	Normalized difference infrared index
NDVI	Normalized difference vegetation index
OHM	Object height model
PRF	Pulse repetition frequency
RMSE	Root mean square error
RTK	Real time kinematic
SLU	Sveriges Lantbruksuniversitet (Swedish University of Agricultural Sciences)
SPOT	Satellite Pour l'Observation de la Terre (Satellite for observation of Earth)
TIN	Triangular irregular network
VCC	Vertical canopy cover
VR	Vegetation ratio

1 Introduction

The term “remote sensing” was introduced in the 1960s. The general term used before that was aerial photography, but with new methods and technology, a new term was established. Aerial photographing was tested already at the end of the 1880s using balloons and kites to lift a camera into the air. About 70 years later, the first satellite image was acquired in 1960 by the US military (Day *et al.*, 1998). Satellite images were acquired on a regular basis and made it possible to monitor changes. Civilian use of satellite images to study earth resources started with the first Landsat satellite in 1972. This was preceded by testing of multispectral scanner systems carried by aircrafts (Swain & Davis, 1978).

Airborne laser scanning (ALS) was introduced in the 1980s, but first became commercial in the mid-1990s. The principle of ALS is described here in a simplified way. The ALS instrument is mounted on an airplane or helicopter where the sensor’s position and pointing direction are continuously recorded using GPS (Global Positioning System) and IMU (inertial measurement unit). A short laser pulse is emitted and the time it takes to be reflected back to the sensor from the ground, branches, leaves, etc. is measured. A 3D coordinate of a reflected point can then be calculated. This process is repeated at the same time as the platform moves forward in the flying direction and the scan angle is changed. Thousands of pulses are emitted every second and a point cloud of 3D coordinates of reflected positions is created. For a more thorough description of the principles of ALS, the reader is referred to Shan & Toth (2009), Lindberg (2012), and can be compared to the principles of photogrammetry in Kraus & Pfeifer (1998).

The development of laser scanners has been rapid and the recent scanners on the market can have scan frequencies around 500 kHz and can record the full waveform of the returned laser pulse. At the time of writing this thesis, Lantmäteriet is scanning all of Sweden (450,295 km^2) using ALS. The density

is at least 0.5 points/m^2. Due to the rapid technological development, it is also of interest to conduct research using higher point density data which is expected to be standard data in the future.

Laser metrics can be calculated from the ALS points and used for estimation of vegetation properties. The ALS point cloud is first classified into ground and non-ground using automatic methods (e.g., Kraus & Pfeifer, 1998; Axelsson, 1999, 2000). A digital elevation model (DEM) representing the ground is then calculated from the ALS points classified as ground. The height above ground of the non-ground points is calculated by subtracting the elevation of each point by the ground DEM. Laser metrics that characterize the vegetation can be calculated for a sample plot or grid cell. Examples of metrics are height percentiles and vegetation ratio. Height percentiles, giving a measure of vegetation height, are calculated from the distribution of all height values above a threshold (e.g., threshold = 1 m). The vegetation ratio, giving a measure of vegetation density, is the proportion of all laser returns that are above the threshold.

1.1 Background and motivation of the studies

Airborne laser scanning has been used for some time to monitor state and changes in forestry (Næsset *et al.*, 2004), but there are fewer studies that investigate the use of ALS for environmental purposes. There is a need to develop methods for monitoring of changes in the forest-tundra ecotone, afforestation of pasture land, and windthrown trees, for example. The papers in this thesis are conducted in three vegetation types: alpine forest, hemi-boreal forest, and pasture land.

Methods for ALS remote sensing for the alpine forests and hemi-boreal forest are in general the same, but the mosaic patterned forest in the mountains requires robust models (paper I) when predicting forest variables. In this thesis, the term "forest-tundra ecotone" is defined as the transition zone where sub-alpine forest and alpine tundra meet (Clements, 1936; Payette *et al.*, 2001). There has been a growing interest in monitoring the forest-tundra ecotone, especially the tree line, which is expected to change with a warmer climate (Kupfer & Cairns, 1996; Kullman, 1998, 2010). In addition to tree line changes, an increase in the biomass of the forest-tundra ecotone can be expected (Tømmervik *et al.*, 2009; Hedenås *et al.*, 2011; Rundqvist *et al.*, 2011). The Arctic Climate Impact Assessment report (ACIA, 2004) states that the arctic average temperature has risen almost twice the rate as the rest of the world in the past few decades. In addition to climate, the tree line is also influenced by other factors such as browsing by moose and reindeer, human

activities and insect attacks (Holtmeier & Broll, 2005; Post & Pedersen, 2008; Olofsson *et al.*, 2009; Hofgaard *et al.*, 2010; Aune *et al.*, 2011; Van Bogaert *et al.*, 2011). Callaghan *et al.* (2002) presented a summary of studies defining the tree line. The conclusion stated that there was a clear need for rationalization of the definitions, but that the task was not trivial. Callaghan *et al.* also states that many studies are based on the term "line", but many characteristics of the forest-tundra ecotone are better characterized by 2- or 3-dimensional patterns. In paper I in this thesis, an area based method is used to create a spatially complete coverage map of above ground biomass in the forest-tundra ecotone. This map can then be used to assess changes by taking the difference between wall-to-wall biomass predictions from two time-points.

Vegetation maps of the forest-tundra ecotone have previously been created by manual photo interpretation. The use of optical satellite images to automatically classify alpine vegetation has also been evaluated (e.g., Reese, 2011). The addition of topography (e.g., slope, elevation, aspect) to satellite images increases the classification accuracy of some alpine vegetation types (Edenius *et al.*, 2003; Reese, 2011). Some alpine vegetation classes, for instance willow, may be confused with other classes due to spectral overlap and similar topographical niches. Therefore, it is of interest to investigate whether classification accuracy could be improved by including laser metrics from ALS.

Series of ALS data start to become available and future multi-temporal data will likely be collected with various point densities, scanning systems, and system parameters, among other characteristics. Efficient calibration methods are needed to perform monitoring or detection of changes using multi-temporal ALS data. In paper III in this thesis, a method to calibrate laser metrics from two different ALS systems was developed and used to detect local changes that differ from the normal development of the landscape.

Early stages of afforestation of pasture lands is difficult to monitor with aerial photos or optical satellite images due to the often tall surrounding grass that makes it difficult to distinguish small newly established trees. Information on afforestation is typically needed for arable land where farmers receive subsidies from the European Union to keep pasture land open or for nature reserves that should preserve certain species and landscape characteristics. Similar needs for detecting new trees also exist for climate related monitoring, such as control of afforestation and reforestation within the REDD+ framework (GOFC-GOLD, 2012). Monitoring the establishment of small trees in arable land is a difficult task, and is similar to the detection of pioneer trees in the forest-tundra ecotone for which some ALS studies exist (e.g., Næsset & Nelson, 2007; Næsset, 2009b; Thieme *et al.*, 2011; Nyström *et al.*, 2012, 2013;

Stumberg *et al.*, 2012). No previous studies have been found which have been conducted in agricultural grasslands using ALS to detect afforestation. It is therefore of interest to examine the minimum level of change in this landscape that can be measured using ALS.

Dead wood in the form of logs from windthrown trees is a valuable resource for biodiversity in forest ecosystems (Bouget & Duelli, 2004; Jonsson *et al.*, 2005). The large number of windthrown trees usually occurring after major storms might, however, sustain large populations of insects that could impose a danger to the remaining living forest (Martikainen *et al.*, 1999). Forest managers would be aided by remote sensing methods which could detect the location of recent windthrown trees. For ecosystem management, as well as for carbon accounting, there is a need for efficient statistical methods for surveying the amount of dead wood logs.

It has been shown that radar as well as optical images acquired from aircrafts or satellites can be used to find areas where many trees have fallen. It is however difficult to find scattered windthrown trees located under a tree canopy from optical satellite data or aerial photos acquired from standard altitudes (i.e., 4,000–5,000 m a.g.l.). The few previous studies detecting windthrown trees on the ground using ALS have been conducted at test sites with tree diameters at breast height (DBH) greater than 300 mm or conducted in areas with low canopy cover. Thus it is motivated to study how well windthrown trees could be detected in Scandinavian forest conditions using ALS data.

1.2 Objectives

The objective of this thesis is to develop methods for mapping and monitoring vegetation using ALS data. The specific objectives for paper I-V are:

I (1) Investigate prediction accuracy of above ground tree biomass, maximum tree height, and vertical canopy cover of mountain birch forest in the forest-tundra ecotone when using models developed from field surveyed sample plot data and corresponding ALS data, (2) compare the results from two different ALS acquisitions with different point densities, flying altitudes, and scanner types, and (3) apply the developed model for above ground tree biomass to calculate complete predictions over the whole study area.

II (1) Classify alpine and subalpine vegetation using a combination of optical satellite data, elevation derivatives, and laser metrics, (2) compare the

accuracy of classification using the different input data, and (3) assess the importance of the individual input variables for their utility in classifying the alpine vegetation types.

III (1) Validate the effect of a histogram matching algorithm when comparing two ALS datasets, and (2) identify metrics from ALS data that are efficient for detecting changes of vegetation in the sub-alpine tree line ecotone using supervised classification.

IV (1) Possibility to measure heights of newly established trees (0.3–2.6 m) in former pasture land using ALS acquired from a single scanning occasion, (2) estimate height change of newly established trees using ALS data acquired from two different scanning occasions, and (3) classify the trees into three classes: unchanged, partly changed and removed tree.

V (1) Develop a method for enhancing the appearance of windthrown trees in a difference elevation model derived from two elevation models, (2) automatically detect windthrown trees in the difference elevation model, and (3) evaluate the results at individual tree level and for 40 m × 40 m grid cells using a complete field survey of windthrown trees in the study area.

2 Literature review

This literature review is divided into four sections. The first section is a review of remote sensing studies in the forest-tundra ecotone with an emphasis on results where ALS has been used. The subsequent section is about change detection methods mainly using ALS. There is also a brief overview of change detection with other remote sensing techniques. The third and fourth sections also provide a review of change detection, but with a focus on two specific applications: remote sensing of afforestation and detection of windthrown trees.

2.1 Remote sensing of the forest-tundra ecotone

The many definitions of the tree line (Callaghan *et al.*, 2002) make it difficult to monitor changes by comparing with previous studies. Field methods to record the tree line have been used for a long time. Kullman (1986) located the uppermost individual of each species with a minimum height of 2 m at a specific location and defined its elevation as the tree line. Large changes in the tree line could then occur when a new tree taller than 2 m was found. Rundqvist *et al.* (2011) compared three 50 m × 50 m plots in the forest-tundra ecotone over a 34-year period and found a substantial increase of shrub and tree (<35 mm DBH) coverage. The reader is referred to Callaghan *et al.* (2002) and Van Bogaert (2010) for more information about field methods.

Remote sensing can offer spatially complete predictions of areas. Aerial photograph interpretation is impractical and dependent on the interpreter when mapping the tree line (Heiskanen *et al.*, 2008). Reese (2011) used optical satellite images to classify alpine vegetation in ten classes with 72.9% overall classification accuracy, where overall accuracy is defined according to Congalton (1991). Optical satellite data can be used for large area overviews, but will not provide a detailed assessment for the structure, height, and biomass

of the forest-tundra ecotone (Allen & Walsh, 1996; Ranson *et al.*, 2004; Heiskanen, 2006a; b; Hill *et al.*, 2007; Heiskanen & Kivinen, 2008; Weiss & Walsh, 2009; Zhang *et al.*, 2009). ALS data will in comparison with optical satellite data provide a better spatial resolution and in particular also data about the 3D structure of the vegetation.

ALS has been proven to measure height and density of vegetation with high precision and accuracy (Hyyppä *et al.*, 2008). There are two main methods used to estimate forest properties: the individual tree method (e.g., Brandtberg, 1999; Hyyppä & Inkinen, 1999; Ziegler *et al.*, 2000; Hyyppä *et al.*, 2001; Persson *et al.*, 2002) and the area based method (Magnussen & Boudewyn, 1998; Næsset & Bjerknes, 2001; Næsset, 2002). Hyyppä *et al.* (2008) presented advantages and disadvantages with the two methods, for example, the single tree method requires higher point density data, but there is less need for extensive reference data. Yu *et al.* (2010) compared area based and individual tree methods at plot level using the same datasets (point density 2.6 m^{-2}). The study indicated that the root mean squared errors (RMSE) for mean height, mean diameter, and volume were similar.

The FAO definition of forest is based on height and density of vegetation (FAO, 2004). The definition reads "land spanning more than 0.5 hectares with trees higher than 5 meters and a canopy cover of more than 10 percent, or trees able to reach these thresholds *in situ*". ALS has large potential to monitor changes of forest, as defined by FAO, as heights and canopy cover can directly be calculated from the point cloud. Lindgren (2012) classified forest, as defined by FAO, using ALS data over an 875 km^2 area in the forest-tundra ecotone in northern Sweden. Lindgren achieved an overall classification accuracy of 92% using 461 field plots.

Rees (2007) used low density ALS data (pulse density 0.25 m^{-2}) to detect the existence of trees in a 120 km^2 forest-tundra ecotone in northern Norway. Rees created a map of forest regions where the definition of forest required trees to be taller than 2 m and have adjacent trees less than 10 m away. No accuracy assessment of the results was done though.

Næsset and Nelson (2007) evaluated how well pioneer trees could be detected on a mountain ridge in southeastern Norway using high-resolution ALS data (pulse density 7.7 m^{-2}) and three different terrain models. A tree was considered to be found if there was a return with a height value larger than zero inside the field measured tree polygon. Regardless of the terrain model used, at least 91% of all trees taller than 1 m were found. The smoothest terrain model resulted in the highest success in tree detection, 42% for trees smaller than 1 m and 97% for trees taller than 1 m. A high commission error of 1,142% for trees was reported when using the smoothest terrain model though. They also

suggested that multi-temporal data could reduce the commission errors as terrain objects will not have changed in height.

Hollaus *et al.* (2007) mapped stem volume for a 128 km^2 large mountainous area in Austria using ALS data from 2002 and 2003 with a point density of 0.9 m^{-2} and 2.7 m^{-2}, respectively. A relative RMSE of 22.9% was achieved for stem volume using a regression model including laser metrics and trained with field data from 103 sample plots. They also tested the use of reduced point density data (0.3 m^{-2}) and achieved only slightly higher relative RMSE (24.7%).

Næsset (2009b) evaluated how properties of the terrain model, choice of sensor, and flight settings influenced the detection and height estimation of small trees in the alpine tree line. A subsample of 342 trees from the study by Næsset and Nelson (2007) was used. Four ALS datasets were aquired with two different instruments, different flying altitudes, and different pulse repetition frequencies (PRF). The combinations were (flying altitude / PRF) 700 m / 100 kHz, 700 m / 125 kHz, 700 m / 166 kHz, and 1,130 m / 166 kHz. An Optech ALTM 3100C sensor was used for the first acquisition and Optech ALTM Gemini for the others. The average point density ranged between 7.7 m^{-2} and 11.9 m^{-2}. A tree was considered to be detected if any return was above zero height within a circular polygon around the field measured coordinate of the tree. The general result was that the detection rate was lowest using ALS data acquired at 700 m flying altitude and PRF 100 kHz whereas the smoothest terrain model (iteration angle 6°) yielded the highest detection rate. For all trees > 1 m, the detection rate was between 93% and 100% regardless of ALS acquisition and terrain model. The corresponding numbers for trees < 1 m ranged from 29% to 61%. The highest commission errors (6,838–8,948%) were found for flying altitude 700 m and PRF 166 kHz and the lowest (709–2,374%) for flying altitude 700 m and PRF 100 kHz. The most likely reason for the higher commission errors at 166 kHz than 100 kHz is the lower precision of the laser ranging measurements at higher PRF causing higher variation of the height returns and therefore more returns appearing to have a postivie height. When estimating height, an underestimation was found ranging between 0.35 m and 0.55 m for the smallest trees (< 1 m) and between 0.99 m to 1.42 m for the tallest trees (> 3 m). Næsset's conclusion was that ALS can potentially detect almost all trees taller than 1 m in the tree line and the flight and sensor properties were all equally well suited. For trees < 1 m though, there were significant differences in the flight and sensor properties.

Jochem *et al.* (2011) used a semi-empirical model to estimate above ground biomass (AGB) of spruce dominated alpine forest in Austria using ALS data with point densities between 0.9 m^{-2} and 2.7 m^{-2}. The semi-empirical model

was first developed by Hollaus *et al.* (2009) to be a robust model to estimate growing stock in alpine forests. In the study by Jochem *et al.*, AGB was expressed as a linear function of canopy volume calculated using 196 sample plots with 12 m radius. The canopy volume was calculated from the height above ground of the first ALS returns. Jochem *et al.* extended the semi-empirical model with three parameters describing the transparency of the canopies. The results showed that the semi-empirical approach by Hollaus *et al.* (2009) could also be used for AGB estimation (standard deviation 35.8%), but the canopy surface transparency extension did not improve R^2 significantly.

Thieme *et al.* (2011) used ALS data with pulse density of 6.8–8.5 m^{-2} to detect single trees in the forest-tundra ecotone in Norway. They used the field measured coordinate to evaluate if small trees could be detected or not using ALS data. If the ALS points within the field measured individual tree crown polygons had a height greater than zero, the tree was counted as successfully detected. The detection rate for trees taller than 1 m was 90%, but for trees shorter than 1 m the corresponding value was 49%.

Stumberg *et.al.* (2012) classified ALS data with pulse density of 6.8 m^{-2} as tree and non-tree returns in the forest-tundra ecotone in Norway. The field data consisted of tree height and crown area of 524 trees with heights from 0.04 m to 7.80 m. Training data, consisting of 2,323 tree and 27,487 non-tree returns, was created using the tree crown polygons. As discriminators they used the laser return's height and intensity, the Voronoi area, and the terrain variables aspect and slope. The overall accuracy was over 93% irrespective of classification method (i.e., generalized linear models and support vector machines). Class specific accuracies were not presented for the two classes (tree and non-tree).

Ørka *et al.* (2012) successfully integrated strip samples of ALS (pulse density 2.7 m^{-2}) with Landsat imagery to delineate the subalpine zone (3,660 km^2) in Hedmark county in Norway. Three classes, forest, alpine, and subalpine zone, were delineated using height and canopy cover calculated from the ALS data. The overall classification accuracy of the three classes using binomial logistic regression and alpha-cuts was 69%. Ørka *et al.* also identified the tree and forest line for specific regions using only ALS data. The predicted lines delineating the three classes showed a good correspondence with the field measurements, but four of the 26 field locations did not have a satisfactory match.

Coops *et al.* (2013) investigated the dual role of remote sensing and physiological modeling when characterizing the alpine tree line in Switzerland. ALS data were collected in September 2010 with a point density of 10 m^{-2}. The Physiological Principles in Predicting Growth (3-PG) model was used to assess

the importance of seasonal variations on four climatically related variables that impose non-linear constraints on photosynthesis (Landsberg & Waring, 1997). The ALS data were used to map tree height and stand density along a series of altitudinal gradients. A strong relationship between field measured tree height and ALS tree height was found (R^2 = 0.85, RMSE = 0.70 m). The 3-PG model showed that the spring and fall temperatures explain most of the difference along the altitudinal zones. The two methods give complementary information on the tree line location and if combined they provide further understanding of potentially endangered forest-grassland transition zones.

To summarize the use of ALS in the forest-tundra ecotone, the studies can be categorized into detection of single pioneer trees (Næsset & Nelson, 2007; Næsset, 2009b; Thieme *et al.*, 2011; Stumberg *et al.*, 2012), delineation of the tree line (Ørka *et al.*, 2012), and large area mapping of forest, volume, or biomass (Hollaus *et al.*, 2007; Rees, 2007; Jochem *et al.*, 2011; Coops *et al.*, 2013). A large number of commission errors have been noticed when detecting small pioneer trees (Næsset & Nelson, 2007; Næsset, 2009b) but on the other hand, the use of an area based approach will in most cases not give information about the pioneer trees on the tundra because of their relatively small size. However, none of the previous studies have been conducted in mountain birch dominated forests and mapped height, biomass, and canopy cover of this forest type.

2.2 Methods for change detection

Optical images from satellites have been used to detect changes of forest (Balzter *et al.*, 2003; Donoghue *et al.*, 2004; Lu *et al.*, 2004), but the spectral signal from trees is driven mainly by the shadow patterns caused by the trees as well as the particular tree species and field layer reflectance. In addition, the area to be detected as a change needs to be at least a few pixels in size in order to be detected as a changed area. For detection of changes, ALS has the advantage that it gives information about vegetation height and density, but on the other hand, does not provide spectral information. There are still problems that need to be solved when using ALS for change detection, for example, repeatability (i.e., achieving comparable measurements when flying over the same area a second time). Stable laser metrics are important when calculating change, otherwise anomalies in the change estimations might occur.

One approach for detection of changes using ALS data is to detect objects in data, for example, using image analysis methods applied on rasterized ALS data, followed by classification and estimation of attributes for the detected objects. One advantage with this approach is that precise estimates are

possible, for example the removal of an individual tree can be detected. On the other hand, in practice, not all objects can be detected, which need to be considered in the analysis (e.g., using statistical models). Another approach is to use area based change detection methods where laser metrics are calculated within raster cells with the size of a field plot. These methods are very sensitive to system parameter settings, though. Often different systems are used for repeated ALS data acquisitions and the differences between laser metrics from two time points are therefore not only a result of vegetation change. This problem can be solved either with relative calibration methods or by calibrating with field samples. So far, most ALS studies have used the field sample calibration. Relative calibration methods have earlier been developed for analysis of optical satellite image data (Olsson, 1994; Tokola *et al.*, 1999; Yang & Lo, 2000; Coppin *et al.*, 2004), but no studies have been found where relative calibration methods have been applied on multi-temporal ALS data.

A few studies have investigated the characteristics of ALS data in vegetation and the effect of altering flying altitude, footprint size, PRF, sampling density, and scan angle (Goodwin *et al.*, 2006; Hopkinson, 2007; Næsset, 2009a; Disney *et al.*, 2010). The reproducibility of laser metrics from ALS data collected the same day has also been investigated (Bater *et al.*, 2011).

2.2.1 Reproducibility of measurements

Goodwin *et al.* (2006) investigated the effect of flying altitude and footprint size for ALS in Wedding Bells State Forest in Australia. When comparing the proportion of first/last returns to single returns, the highest flight altitude (3,000 m) had higher proportion of single returns than the lower flight altitudes (1,000 m and 2,000 m), probably because of the reduced returned energy due to higher flight altitude. Canopy heights and canopy covers, however, were not significantly affected by the flying altitude. It was also shown that attributes for individual trees were strongly affected by the point spacing and structural characteristics of the specific sites.

Hopkinson (2007) collected eight ALS acquisitions over the same area in Nova Scotia, Canada to investigate the influence of flying altitude, beam divergence, and PRF. The intensity values of the laser pulses were found to be linearly related ($R^2 = 0.98$) to peak pulse power concentration on the reflecting target. The peak pulse power concentration, as well as the returned intensity, decreases with higher flying altitude, scan angle, beam divergence and PRF. It was concluded that the laser peak pulse power concentration was the most important factor in the determination of returned intensity and also caused systematic variations in the canopy height distribution if varied. With lower

peak pulse power concentration, the penetration was slightly reduced for short canopy foliage and increased penetration in tall canopy foliage. It was suggested that calibration models for vegetation characterization should be developed which would also take into account the variations in laser pulse power peak concentration if data were collected with different survey settings.

Næsset (2009a) concluded that different ALS sensors, flying altitudes and PRFs affect height-related as well as canopy density-related metrics. Higher flying altitude tends to give higher values for the height metrics for both single+first and last returns. Height metrics derived from the last returns also tend to be less stable between the flying altitudes than the metrics derived from the single+first returns. Lower PRF tend to produce an upward shift of the canopy heights compared to higher PRF, which results in higher values for height metrics and density metrics. The precision seems to be relatively stable when estimating forestry variables, such as mean tree height and timber volume, using different sensors, flying altitudes, and PRF, but significant differences in mean values were observed. This study presented a mean difference for timber volume of up to 10.7% and up to 2.5% for mean height.

Disney *et al.* (2010) simulated the impact of ALS system and survey characteristics over pine and birch forest. Detailed models of Scots pine and Downy birch were used to simulate the laser returns. Signal triggering method, foot print size, sampling density, and scan angle affected the height of returns in the tree crowns and differences could also be observed for the two species.

Bater *et al.* (2011) collected four ALS acquisitions from the same day over a forested area on Vancouver Island to validate the reproducibility of laser metrics. The four overlapping acquisitions were collected with identical sensor and survey parameters and covered a 3 km transect with a pulse density of 2 m^{-2}. The number of returns and the number of first returns were significantly different between the four flight lines. Height metrics calculated only from first returns showed no statistical difference, except for maximum height. The estimate of understory cover was not significantly different, but the estimate of overstory cover was significantly different. The mean and standard deviation of returned intensity were also significantly different, as well as all height metrics calculated from last return data.

2.2.2 Area based change detection

Næsset & Gobakken (2005) estimated forest growth in a boreal forest in southeastern Norway by comparing two independent predictions based on ALS datasets that were acquired two years apart. The average pulse density in the 1999 data was 1.2 m^{-2} and in the 2001 data it was 0.9 m^{-2}. Out of the 54 laser metrics, 45 changed their value significantly due to forest growth. The upper

height percentiles, however, had a larger increase in their values than the field measured height growth. For example, the 90th height percentile increased by 0.4–1.3 m and the field measured mean height growth on the sample plots was 0.2–0.9 m. Mean tree height, basal area, and volume were estimated for respective acquisition using regression. Predictions from the ALS data showed significant growth in all three variables, but the predictions were biased and had low precision. The results were better for young forest than mature forest and it was clear that first returns were better predictors of forest growth than last returns. It was also noted that some metrics were not suitable for growth estimation, such as maximum height, as it tended to be less stable.

Solberg *et al.* (2006) mapped changes in leaf area index (LAI) due to insect attacks by using ALS data calibrated to field measurements. Three ALS acquisitions were performed in May, July, and September 2005 with a pulse density varying between 3.1 and 9.8 m^{-2}. LAI was determined in 20 field plots using the LAI-2000 instrument. Gap fraction was estimated from the ALS data as the ratio of canopy returns to the total number of returns. Different linear regression models of field measured LAI were estimated based on either first or last return data. The strongest relationship between the field measurements and the ALS data was found for the first return data (R^2 = 0.93). When comparing the mean of predicted LAI from the three acquisitions in pure pine stands, the LAI values were 0.94, 0.96, and 0.96 (in time acquisition order), which indicated an increase in LAI during the summer despite the insect attack.

Yu *et al.* (2008) compared three methods for plot wise estimation of mean tree height and volume growth for 33 sample plots in southern Finland. The ALS datasets were the same as in Yu *et al.* (2005). Variables for the trees were calculated using data inside a cylinder with its center being the field measured tree coordinate with a radius based on the height of the tree. Three different types of variables were extracted for the height change estimation: difference in maximum height, digital surface model (DSM) differences, and difference in height percentiles (50th, 60th, 70th, 80th, 85th, 90th, and 95th). Regression models for mean tree height and volume growth were estimated for the single best predictor for each method and by selecting predictors from all methods. The best method to estimate mean tree height growth was the maximum tree height differencing method (adjusted R^2 = 0.84). For volume growth estimation, the best method was the DSM differencing method (adjusted R^2 = 0.56). When combining the methods and selecting the best predictor, there was no improvement for the mean tree height growth estimation, while for volume growth the adjusted R^2 value increased from 0.56 to 0.75.

Hopkinson *et al.* (2008) evaluated the estimation of plot level mean tree height growth using four ALS acquisitions of a pine plantation in Toronto,

Canada. ALS data were collected in year 2000, 2002, 2004, and 2005 with a point density around 3 m^{-2}. Field measured height change of 126 trees within 19 plots was collected in 2002 and 2005. The 90^{th}, 95^{th}, and 100^{th} height percentiles all had high correlation with field measured tree height. Although the 100^{th} height percentile provided the most robust overall direct estimate of field measured forest growth, most ALS-based methods underestimated the growth. The growth rate estimate was around 0.32 m/year using the 100^{th} height percentile and around 0.4 m/year in the field measurements. The RMSE of field measured height change and the 100^{th} height percentile difference was 0.58 m.

Vepakomma *et al.* (2008) used multi-temporal ALS data to map canopy gaps of a 6.0 km^2 area in southern Québec, Canada. The ALS data were collected in 1998 and 2003, with a pulse density of 0.3 m^{-2} and 3 m^{-2}, respectively. Horizontal shifts were checked visually by studying, for example, hill shading and trends in slope between the DEMs (with 0.5 m cell size) created from each acquisition; no horizontal shifts were found. Elevation differences were also checked by comparing the elevation for patches of bare ground which resulted in lowering the 1998 data 22 cm in elevation. The gaps were automatically delineated in canopy height models (CHMs) with a 0.25 m cell size using an object-based technique. Accuracy assessment was done only for the 2003 data using four randomly located line transects with a total length of 980 m. Of the total 29 gaps, 28 were found (with gaps as small as 5 m^2 identified), and 73% of the gap length was identified. It was observed that the total area of gaps had decreased from 200 ha to 181 ha.

Vastaranta *et al*. (2012) detected snow-damaged trees in southern Finland using the difference in ALS measured canopy heights. The pulse density ranged between 7–12 m^{-2} for the ALS datasets collected in 2006, 2007, and 2010. The snow-damaged trees were detected by applying thresholds to height difference and area of damage between two CHMs. The overall detection rate was 66% which represented 81% of the total stem volume of snow damaged trees. At plot level, the omission error was 19–75% and the commission error 0–21%.

Hudak *et al.* (2012) estimated biomass change and carbon flux in northern Idaho, USA using ALS data from 2003 and 2009. The 2003 data had a point density of 0.4 m^{-2} and the 2009 data 12 m^{-2}. They recommended four points to consider when assessing biomass change using multiple ALS datasets. First was to beware of the difference in the ALS sensors and to use metrics that are stable for both low- and high point densities, such as mean canopy height. Second, field plots need to represent the landscape in an unbiased way. Third, field plot centers should be measured with high precision and the plot center

marked permanently. Fourth, consistency is required for measuring biomass of field plots. Biomass models were developed separately for the two datasets using Random Forest (Breiman, 2001) with 62 candidate laser metrics. The root mean square difference was 92.8 Mg/ha for the 2003 acquisition and 101.9 Mg/ha for the 2009 acquisition. The biomass change, which was calculated by plot wise subtraction of the two independent predictions, was more variable than the two independent predictions, but still significantly correlated.

Bollandsås *et al.* (2013) tested three approaches for estimation of biomass change between two ALS acquisitions in the Norwegian mountains. The first approach was simply the difference between biomass predicted from the two ALS acquisitions. The second approach used change in different variables between the ALS acquisitions to model biomass change. The third approach modeled relative change in biomass. The two ALS acquisitions were collected at two time points (four growth seasons apart) and with different scanners. The first scanning had a point density of 3.4 m^{-2} and the second 4.7 m^{-2}. The two direct approaches (second and third) resulted in lower RMSE than predicting at two occasions, probably because the results were affected by only one model error.

Næsset *et al.* (2013) estimated 11 years of change in forest biomass in an 853 ha area in southeastern Norway using a sampling approach where ALS data were used as auxiliary information in a model-assisted approach. The pulse density was 1.2 m^{-2} in the 1999 data and 7.3 m^{-2} in the 2010 ALS data. The 176 sample plots used were located using a stratified systematic design. Three different models were used: first, directly modelling the change in biomass, second, modelling the change in biomass by a system of models, and third, modelling the change in biomass by separate models at each time-point. They reported a 57% reduced standard error of the overall net change in biomass compared to using only the field surveyed data. In general, the direct approach (first) resulted in better precision than the two other approaches (second and third), which is consistent with the finding of Bollandsås *et al.* (2013).

2.2.3 Object based change detection

Hyyppä *et al.* (2003) was the first study that demonstrated that multi-temporal ALS data could be used to measure forest growth. The two ALS acquisitions used were collected over a boreal forest in southern Finland in September 1998 and June 2000, both with a point density of 10 m^{-2}. A tree-to-tree matching algorithm was used to calculate the height growth for the individual trees. The standard error was less than 5 cm when estimating height growth at stand level.

At individual tree level, the mean height growth deviated on average 28 cm from the field measured height growth of the 15 reference trees. The major factors affecting the tree height estimates were errors in the terrain model, segmentation (tree objects), linking of the trees, and small trees that were not identified in the ALS data.

Yu *et al.* (2004) automatically detected harvested trees and estimated forest growth between two ALS acquisitions in southern Finland (same two acquisitions as used in Hyyppä *et al.* (2003)). Systematic and random errors were found in the ground DEMs created and DEM compensation was performed to remove these errors. This was done to make sure that the terrain was unchanged between the two acquisitions which could cause false canopy height changes. Trees were linked to calculate height growth of individual trees. All trees were not successfully linked in the 20 stands used in the study. The percentage of correct links per stand ranged from 39% to 70%. Mean height growth at plot level was estimated with a precision of 10–15 cm and about 5 cm at stand level. Sixty-one of the 83 field checked harvested trees were automatically and correctly detected. It was mainly the smaller harvested trees that were not detected. It was also noted that many of the individual tree segments included two or more trees, which could have affected the results.

St-Onge and Vepakomma (2004) used ALS data acquired in 1998 and 2003 to detect fallen trees and tree growth within a 6.8 ha study site in Québec, Canada. The pulse density of the 1998 data was 0.3 m^{-2} and for the 2003 data it was 3 m^{-2}. The same ground DEM (from the 2003 data) was used for both years to avoid false canopy height changes. The 1998 data were adjusted in height by comparing the ground returns from the two datasets. Three ways of measuring height growth were evaluated: at tree crown level by delineating the crowns manually, tree crown level with automatic delineation, and at area level in 20 m × 20 m windows. The manually delineated crowns resulted in height growths close to the observed values and similar results were obtained for the automatically delineated crowns. The area level height growth estimates worked well for hardwoods, but not for softwoods. Canopy gaps were detected by locating points where the canopy height (CH) was higher than 10 m in the 1998 data and CH less than 10 m in the 2003 data. In the study site, 88 new gaps were found with an overall accuracy of 96% when comparing with visually interpreted images from Ikonos, Quickbird and videography (collected from an airplane flying at 1890 m a.g.l.). The gap commission error was only 8%.

Yu *et al.* (2005) estimated growth of individual trees using ALS data from September 1998, June 2000 and May 2003. The point density was around 10 m^{-2} for all three scanning occasions. Field height measurements of 153

pines were done in August 2002 and November 2004. Annual growth was estimated by field measuring three to six consecutive shoots below the top of the tree, which resulted in an accuracy of 10–15 cm. The field measured coordinate of each tree was used to extract the maximum height value from the ALS data within a cylinder based on the height of the tree. The tree height growth was calculated as the difference of the extracted maximum heights from the ALS data. RMSE of individual tree growth between 1998 and 2003 was 45 cm with a bias of 10 cm which implies an overestimation in the ALS data. Between 1998 and 2000 the RMSE was 46 cm and bias was 0 cm and between 2000 and 2003 the RMSE was 38 cm and the bias was 11 cm. It should be noted that the scanning in 2003 used a different scanner than the two previous acquisitions, which could be a reason for the bias between the two later scannings.

Yu *et al.* (2006) compared different methods for height growth estimation of individual trees in southern Finland using ALS data from September 1998 and May 2003. The point density was around 10 m^{-2} for both acquisitions. Field measurements of 82 pines were collected in August 2002 and November 2004. Five to seven consecutive shoots below the top of the trees were measured to estimate the annual growth. Three different types of variables were extracted for the height change estimation: difference in maximum height, mean or median of DSM differences, and difference in height percentiles (85^{th}, 90^{th}, and 95^{th}). Treetop locations were sought in the ALS data in a close neighborhood from the field measured coordinates of the trees. The treetop locations were used as the center location of the cylinder in which ALS points were extracted of each individual tree. The lowest RMSE (43 cm) was achieved for the method which used the difference in maximum height. The other methods resulted in RMSEs ranging between 48 cm and 78 cm. A new tree-to-tree finding algorithm was also developed. When tested on 1,644 field measured trees, the number of matched trees divided by total number of trees measured in the field was 60.8%.

2.3 Remote sensing of afforestation

Afforestation has not been widely studied previously using remote sensing. There are studies classifying shrub vegetation (Waser *et al.*, 2008b; Hellesen & Matikainen, 2013) and estimating biomass and volume of shrub (Estornell *et al.*, 2012a; b), but very few studies have monitored change (Waser *et al.*, 2008a). Waser *et al.* (2008a) used DSMs from aerial photos to estimate shrub encroachment between 1997 and 2002. Waser *et al.* (2008b) used DSMs from aerial photos to generate a probability map of shrub/tree cover in open mire

land in Switzerland. Factors affecting shrub volume estimation in Chiva, Spain were studied using ALS data by Estornell *et al.* (2012a), as well as ALS data and aerial photos by Estornell *et al.* (2012b). Hellesen & Matikainen (2013) showed that classification of trees and shrubs above 1.8 m height, as well as ground and buildings, improved from 82% overall accuracy when using only CIR ortho-photos to 97% when also including ALS data. In this literature review, no studies were found using multi-temporal ALS data to detect changes of small individual trees in agricultural grasslands.

2.4 Detection of windthrown trees

Field based objective survey methods for estimating amount of dead wood have been developed by, for example, Warren & Olsen (1964), Ståhl (1997), Gove *et al.* (1999), Bebber & Thomas (2003), Jordan *et al.* (2004), Gove *et al.* (2005) and Ståhl *et al.* (2010). Such methods are expensive if not combined with other surveys like National Forest Inventories, for example, Fridman & Walheim (2000), or used in multiphase sampling approaches together with remote sensing data.

Aerial photos or optical satellite images can be used to detect areas where many trees have fallen (Wilson & Sader, 2002; Pasher & King, 2009). It is difficult to detect scattered windthrown trees located under a tree canopy from optical satellite data, or from aerial photos acquired from standard altitude (i.e., 4,000–5,000 m above ground). A drawback of using optical satellite images for this purpose is that thinning cuttings cause a similar increase in reflectance as partially windthrown areas, which reduces the usefulness of change detection (Olsson, 1994). Compared to optical satellite data, use of radar data can provide better separation, since windthrown trees tend to increase radar backscatter while removal of trees reduces the backscatter. However, the increase or decrease of backscatter for windthrown forest depends largely on the wavelength used. Promising results have been obtained using the long wavelength airborne radar system CARABAS-II (Fransson *et al.*, 2002; Ulander *et al.*, 2005). The results from CARABAS-II show that detection success depends mainly on the direction of illumination (flight direction), with illumination perpendicular to the windthrown trees giving the strongest backscatter.

Similar to radar, ALS is an active remote sensing technology that penetrates the tree canopies and therefore has potential to find objects close to the ground. Promising results have also been obtained in a few studies for area level estimations of windthrown trees using ALS data (St-Onge & Vepakomma, 2004; Pesonen *et al.*, 2008; Vehmas *et al.*, 2011). St-Onge & Vepakomma

(2004) detected gaps arising after trees had been windthrown. Pesonen *et al.* (2008) estimated downed and standing dead wood volumes at area level using regression models of height and intensity metrics from ALS data calibrated with field measurements. Vehmas *et al.* (2011) detected canopy gaps using ALS data and classified them into five canopy gap classes, including a class of downed dead wood. There are three studies detecting windthrown trees on an individual tree level in high density ALS data (Blanchard *et al.*, 2011; Lindberg *et al.*, 2013; Mücke *et al.*, 2013).

Blanchard *et al.* (2011) used object-based image analysis to classify downed logs in California, USA using gridded ALS data (point density 10.5 m^{-2}). The study area had low canopy cover, bare ground, low-growing shrubs (maximum 0.3 m), and tall trees in the range of 10 m to 60 m in height. Blanchard *et al.* completely or partially classified 73% of 103 downed logs correctly. They also noticed that over-classification occurred in areas where a large number of logs were clustered and in areas with shrub and tree canopies, but no commission errors were presented.

Mücke *et al.* (2013) identified downed trees using small footprint full-waveform ALS data (point density 29.4 m^{-2}, pulse density 10.9 m^{-2}) in eastern Hungary. The field data consisted of 82 downed trees with a minimum diameter of 300 mm. They used a stepwise detection process based on variables such as normalized heights and echo widths to generate a map of downed trees. They detected 75% of the 82 field surveyed trees in the area and had a commission error of 9%.

Lindberg *et al.* (2013) detected windthrown trees in the ALS point cloud (point density 69 m^{-2}) instead of rasterizing the data first. The study area was the same as in paper V in this thesis, Remningstorp, Sweden. A line template matching method was applied directly to the laser point cloud. They detected 41% of the 651 field surveyed downed logs, but had a commission error of 89%.

Honkavaara *et al.* (2013) detected gaps after a winter storm in Finland using a difference of the DSM from ALS and the DSM from matching of aerial photos. The ALS data had a point density of at least 0.5 m^{-2} and was collected in the spring 2008. The aerial photos were collected in January 2012 only a few days after the storm with snow on the ground and low solar elevation angles (5–7°). Areas of change were identified in the difference DSM and classified into areas of change, sparse change and no change. By visually classifying 1 ha areas in the airborne images, the method was evaluated. All areas with more than 10 windthrown trees per hectare were successfully found. Areas with less than 10 fallen trees per hectare were mixed up with unchanged areas and were found with an accuracy of 46%.

The previous studies using ALS data to detect individual dead trees on the ground, with the exception of Lindberg *et al.* (Lindberg *et al.*, 2013), have been done in test sites with minimum diameter breast height (DBH) of 300 mm (Mücke *et al.*, 2013) or conducted in areas with low canopy cover (Blanchard *et al.*, 2011).

3 Material and methods

3.1 Study areas

The study areas are located in Abisko and Remningstorp (Figure 1). The Abisko area in northern Sweden is dominated by mountain birch (*Betula pubescens* ssp. *czerepanovii*) and alpine vegetation. The study area in Remningstorp used in paper IV was a former pasture land and in the later years small alder trees (*Alnus glutinosa*) had established. Paper V was conducted in managed forest in Remningstorp dominated by Norway spruce (*Picea abies*) and Scots pine (*Pinus sylvestris*). Table 1 gives a summary of the study areas.

Table 1. *Summary of the study areas used in the papers.*

Paper	Area	Lat. Long.	Nature type	Field data
I	Abisko	68°20' N, 19°01' E	Mountain forest and alpine vegetation	Systematical grid of 104 plots, 10 m radius
II	Abisko	68°20'N, 18°52' E	Mountain forest and alpine vegetation	Training: 61 clusters of 9 plots, 179 photo interpreted 100 m^2 areas. Validation: 400 photo 100 m^2 areas.
III	Abisko	68°20' N, 19°01' E	Mountain forest and alpine vegetation	43 plots 6 m radius and 53 plots 10m radius
IV	Remningst.	58°29' N, 13°37' E	Abandoned pasture land with small trees	383 trees within 0.3 ha area
V	Remningst.	58°29' N, 13°38' E	Managed hemi-boreal forest	651 windthrown trees within 54 ha area

3.2 Field data

Table 1 gives a summary of the field data used in the papers. The sample plot centers were measured with RTK GPS with sub-dm accuracy, except for paper V where post-processed DGPS produced positioning measurements with errors of several meters.

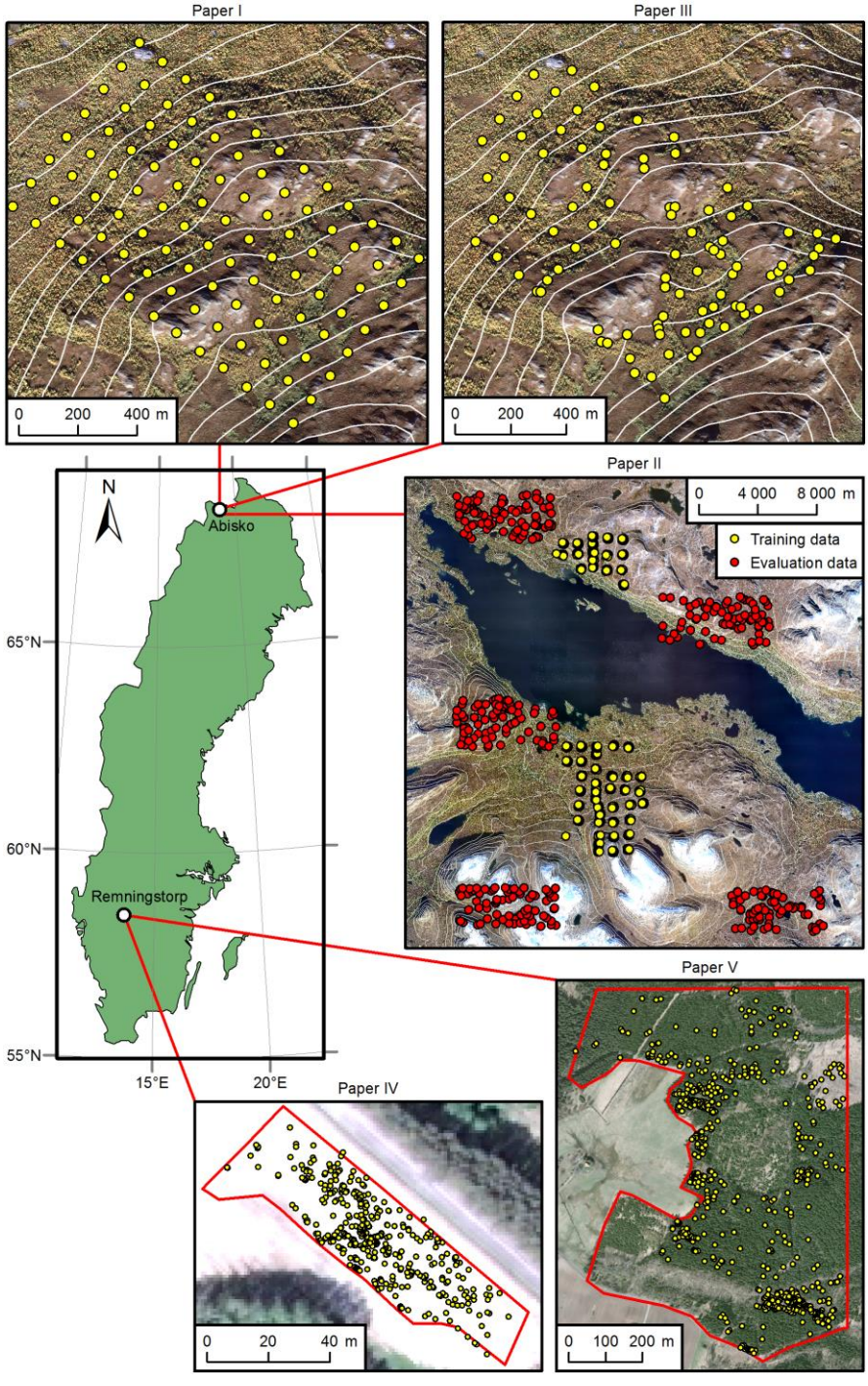

Figure 1. Location of the study areas in Sweden. © Lantmäteriet, i2012/901.

3.2.1 Paper I

In total, 104 sample plots with 10 m radius in a systematic grid with 100 m spacing, covering a 1.3 km × 1.3 km area in the forest-tundra ecotone were field surveyed. For trees taller than 2 m, DBH, canopy extent, and tree height were measured. Above ground biomass was calculated using functions by Dahlberg *et al.* (2004) where DBH and height of the field measured trees were used as input. Photos from the field-work can be seen in Figure 2 and Figure 3.

3.2.2 Paper II

The training data were from a systematic grid of 61 clusters with each cluster consisting of 9 sample plots with 20 m radius and 179 subjectively chosen training samples (single pixel, 10 m × 10 m) that were manually interpreted in stereo aerial photographs. The validation data were selected using an elevation-stratified random design for 400 manually interpreted samples (10 m × 10 m areas) in stereo aerial photographs.

3.2.3 Paper III

In total, 43 sample plots with a 6 m radius were placed in the border zone between mountain forest and tundra. In addition, 53 sample plots, from paper I were used as reference plots, but with a 6 m radius. Changes were simulated by assigning one of the following treatments: (1) reference, no removal of trees, (2) removal of 50% of the total number of trees taller than 1.5 m, and (3) removal of 100% of the total number of trees taller than 1.5 m.

3.2.4 Paper IV

All 383 trees within an area of 2,800 m^2, (marked with red border in Figure 1) were measured. Each tree was positioned and height measured. One of the following treatments was assigned to each tree: leave as reference, cut at root level or cut to half of the height. Figure 4 shows some of the trees in the study area.

3.2.5 Paper V

All windthrown trees (651) lying on the ground within an area of 54 ha (marked with red border in Figure 1) were field surveyed. The following data were collected for each lying tree stem: position, direction, DBH, length, species, height above ground and if the stem was broken or not.

Figure 2. Paper I, measuring height of a mountain birch using a 7 m measuring pole.

Figure 3. Paper III, typical sample plot in the forest next to the tundra.

Figure 4. Paper IV, abandoned pasture land where small alder trees have established.

3.3 Laser data

Table 2 gives an overview of the ALS data used in the papers in this thesis. The TerraScan software (Soininen, 2012) was used to classify the ALS data as ground and non-ground using a progressive triangulated irregular network (TIN) densification method (Axelsson, 1999, 2000).

Table 2. *Overview of the ALS data used in the papers.*

Parameter	Paper V	Paper I, III	Paper I, II, III	Paper IV	Paper IV
Acquisition date	Apr. 24, 2007	Aug. 1, 2008	Aug. 20, 2010	Aug. 29, 2010	Sep. 9, 2010
Scanner model	TopEye MkII	TopEye MkII	Optech ALTM Gemini	TopEye MkIII	TopEye MkIII
Carrier	Helicopter	Helicopter	Fixed wing aircraft	Helicopter	Helicopter
Flight altitude (m a.g.l.)	130	500	1740	200	200
Footprint (m)	0.13	0.5	0.5	0.1	0.1
Pulse repetition frequency (kHz)	50	50	70	160	160
Wave length (nm)	1064	1064	1064	1550	1550
Pulse length (ns)	4	4	6.8	3	3
Scan type	Palmer	Palmer	Oscillating mirror	Rotating mirror	Rotating mirror
Scan width (across flight dir., deg.)	±20	±20	±20	±30	±30
Scan width (along flight dir., deg.)	±14	±14	0	0	0
Points extracted per pulse	≤2	≤2	≤4	≤7	≤7
Point density, mean (m^{-2})	65	6.1	1.4	54	46

3.4 Analysis methods

A digital elevation model (DEM) representing the ground level was calculated using TIN-interpolation of the ground-classified ALS data. Canopy heights (CHs) were calculated by subtracting the ground DEM from the elevation of each laser return. A digital surface model (DSM) was created by assigning the maximum elevation for laser returns classified as non-ground to each grid cell. A normalized DSM (nDSM) was calculated by subtracting the ground DEM from the DSM. In paper I–III, a grid cell size of 0.5 m was used and in paper IV–V, which had higher density ALS data, a grid cell size of 0.1 m was used.

Laser metrics were calculated from the CHs and the nDSM for values above a height threshold (Nilsson, 1996). The height threshold was set depending on the forest type and application. The calculated laser metrics were as follows: height percentiles (H_{10}, H_{20}, …, H_{100}), vertical canopy density metrics (D_0, D_1, …, D_9) according to Næsset and Gobakken (2008), mean height (H_{mean}), standard deviation (H_{sd}), normalized sum of squared heights (H_{sum}), and vegetation ratio (VR). Vegetation ratio was calculated in two ways: first the common way which is by dividing the number of returns above the height threshold with the total number of returns (Hyyppä *et al.*, 2008), and secondly by weighting each ALS point according to the density of surrounding points (developed in paper I). Both ways of calculating the vegetation ratio used either all returns (denoted VR_{all}) or only first returns (denoted VR_{1st}). The point-weighted vegetation ratio is denoted with "pw" subscripted (e.g., $VR_{pw,1st}$). Metrics calculated from nDSM were denoted with nDSM superscripted (e.g., H^{nDSM}) and metrics calculated from CH with CH superscripted (e.g., H^{CH}).

To evaluate the accuracy of classification, an error matrix was calculated (Congalton, 1991). The error matrix is a square array of numbers where the columns usually specify the reference data and the rows show the classification produced using remote sensing data. From the error matrix, user's and producer's accuracy as well as overall accuracy are calculated. Producer's accuracy is the probability that a certain class in the field is correctly classified as such. User's accuracy is the probability that a map element classified as a certain class is indeed that class. The overall accuracy is calculated by dividing the total correct by the total number of reference data samples.

3.4.1 Prediction of tree biomass in the forest–tundra ecotone using airborne laser scanning (paper I)

The area based method (Magnussen & Boudewyn, 1998; Næsset & Bjerknes, 2001; Næsset, 2002) was used in this paper. The laser metrics were calculated

only from CHs and using a height threshold of 1 m. Regression models were developed based on data from the sample plots to predict the following response variables: maximum tree height (MH), above ground tree biomass (AGB) and vertical canopy cover (VCC). Separate models were created for the two datasets, Optech and TopEye. The models were developed to be robust and support the objective of making predictions in the mosaic patterned forest-tundra ecotone. Best subset regression (Lumley and Miller, 2009) was used to select the best laser metrics to explain the response variables. Logarithmic bias was corrected following Holm (1977). Validation was done by calculating RMSE and bias using leave-one-out cross-validation (Weisberg, 1985). Leave-one-out cross-validation is done by using a single observation as validation data and the remaining observations as training data. The process is repeated until all observations have been used once in the validation data. A raster map of AGB with pixel size 10 m × 10 m was created by calculating the developed model for each pixel in the study area.

3.4.2 Combining airborne laser scanning data and optical satellite data for classification of alpine vegetation (paper II)

Laser metrics were calculated in 10 m × 10 m grid cells. A height threshold of 0.2 m was used when calculating metrics from CH and nDSM. The vegetation ratio was calculated using a variable threshold though, from 0.1 m to 1.0 m in 0.1 m increments (example of notation: $VR_{thresh=0.1}$). The standard deviation was also calculated from $VR_{thresh=i}$ where $i = 0.1, 0.2, ..., 1.0$ and denoted $VR_{\sigma(thresh=i)}$. The following elevation derivatives were calculated from the Swedish 50 m grid ground DEM: elevation, slope, aspect, and the Saga wetness index (Böhner *et al.*, 2002). From the SPOT 5 HRG data, the green, red, near infrared, and shortwave infrared bands were used. In addition the normalized difference vegetation index (NDVI; Rouse *et al.*, 1973) and the normalized difference infrared index (NDII) were calculated.

The Random Forest algorithm (Breiman, 2001) was used for the classification. The "varSelRF" package (Diaz-Uriarte, 2010) in R (R Development Core Team, 2010) was used to identify variables contributing most towards building an accurate model. The training data from the systematic clustered field plots had a predominance of dry heath samples and could be considered "imbalanced". A "balanced" training dataset was therefore created by reducing the samples from classes with more than 45 observations using random selection to achieve approximately 40 training samples for these classes. After the most important variables were identified, the classification accuracy was assessed using the evaluation dataset with the following runs: (1) single SPOT 5 data only, (2) SPOT 5 data and elevation derivatives, (3) SPOT

5 data, elevation derivatives and laser metrics, and (4) laser metrics and elevation derivatives.

3.4.3 Change detection of mountain birch using multi-temporal ALS point clouds (paper III)

A height threshold of 0.7 m was used when calculating metrics from CH and nDSM. The lower threshold in this paper was chosen to obtain reliable laser metrics for sample plots with trees around 1.5 m tall while omitting most of the shrub vegetation close to the ground. Laser metrics were calculated in 10 m × 10 m grid cells for an area of 1.8 km^2, covering the study area. The laser metrics inside this area were used to calculate cumulative histograms for each laser metric and acquisition. Histogram matching was used to calibrate the metrics from the two ALS acquisitions to common distributions. The histogram matching routine produced a look up table which was used to transfer the laser metrics from the Optech data to the same distribution as the laser metrics from the TopEye data. For each laser metric calculated from the field plots the look up table was used to calibrate the Optech data. Afforestation was simulated by using the TopEye data as the "after" data and the Optech data as "before" data. The unchanged field reference plots were used to evaluate the similarity of the metrics before and after histogram matching was conducted. The relative RMSE (rRMSE) used in paper III was defined as

$$\mathrm{rRMSE}(k) = \frac{\sqrt{\sum_{i=1}^{n} \frac{\left(T_1(i,k) - T_2(i,k)\right)^2}{n}}}{\bar{T}_{1,2}(k)} \quad (1)$$

The relative bias (rBias) in paper III was defined as

$$\mathrm{rBias}(k) = \frac{\sum_{i=1}^{n}\left(T_1(i,k) - T_2(i,k)\right)}{n\,\bar{T}_{1,2}(k)} \quad (2)$$

where i is the index of the unchanged sample plots, k is the laser metric, $T_1(i,k)$ is laser metric k of sample plot i from the 2008 data and $T_2(i,k)$ is the same laser metric (k) from the same sample plot (i) in the 2010 data, n is the number of unchanged sample plots, and $\bar{T}_{1,2}(k)$ is the mean value of laser metric k, i.e., mean value of $T_1(k)$ and $T_2(k)$.

Linear Discriminant Analysis (LDA) classification was used to evaluate which laser metrics best discriminated the experimentally changed from

unchanged vegetation. The relative differences (equation 3) of the laser metrics were used as explanatory variables.

$$\Delta(i,k) = \frac{T_1(i,k) - T_2(i,k)}{T_1(i,k) + T_2(i,k) + 10^{-15}} \quad (3)$$

The classification was based on either one or a combination of two explanatory variables ($\Delta(i,k)$). Leave-one-out cross-validation was used to calculate classification accuracy using all 96 sample plots.

To evaluate the classification based on laser metrics, sample plots were divided into three change classes, which were also stratified into three density categories depending on the total number of trees taller than 1.5 m.

3.4.4 Detecting afforestation at individual tree level using ALS (paper IV)

All of the following processing was conducted for both dates of ALS data. Models created from the first and second scanning are denoted with subscript 1 and 2, respectively. In contrary to paper I, II, III, and V, an algorithm based on an active surface (Elmqvist, 2000, 2002) was used to produce the DEM which represented the ground. The DSM and nDSM were calculated as described in section 3.4. A difference raster ($nDSM_\Delta$) was calculated by subtracting the second scanning's nDSM ($nDSM_2$) from the first scanning's nDSM ($nDSM_1$). This difference raster ($nDSM_\Delta$) was median filtered with a 3×3 kernel.

The height was estimated to the maximum value from $nDSM_1$ in a 0.3 m radius around the field position of the tree, but no calibration against field data was done. Height change was estimated by subtracting the maximum height within a 0.5 m radius around the field coordinate in $nDSM_1$ and $nDSM_2$. The corresponding field height change was also calculated within a 0.5 m radius around the field coordinate to avoid the problem of taller trees shading a smaller tree.

LDA classification was used to classify the trees into the three categories: reference, 50% removal and 100% removal. The discriminators used were maximum height from $nDSM_1$ and $nDSM_2$ in a 0.3 m radius from the field coordinate. Two different classifications were conducted: using all field measured trees, and using only trees taller than 1 m. Leave-one-out cross-validation was used to assess accuracy.

3.4.5 Detection of windthrown trees using airborne laser scanning (paper V)

Two DEM s were created: first a smooth model created using TerraScan (Soininen, 2012) and secondly a more elastic model created using an active surface (Elmqvist, 2000, 2002; Elmqvist *et al.*, 2001). The two DEMs were subtracted to achieve an object height model (OHM), which is a model

representing objects close to the ground. Template matching was used to identify potential windthrown trees in the OHM. LDA classification was used to reduce the number of falsely detected trees, which typically occurred along roads and streams. The discriminators used in the classification were metrics created from the area of the template in the OHM. Training data for the classification was achieved by manually linking field surveyed trees with the automatically detected trees from the template matching. Falsely detected trees were also identified and used as training data for a non-tree class. The automatically detected trees were linked to field surveyed trees using an algorithm (Olofsson *et al.*, 2008) that maximized a weight calculated from Euclidian distance and difference in direction between the field surveyed tree and the automatically detected tree.

The results were evaluated both at individual tree level and area level. The individual tree results were primarily based on count, but also on tree volume. The area level evaluation was based on a 40 m × 40 m grid covering the study area. In each grid cell, the proportion of correctly detected trees was calculated.

4 Results

4.1 Prediction of tree biomass in the forest–tundra ecotone using airborne laser scanning (paper I)

Multiple linear regression was used to estimate models to predict above ground tree biomass, maximum tree height and vertical canopy cover from ALS data in the forest-tundra ecotone. The denser TopEye data (6.1 points m^{-2}) showed only a small improvement in the predictions compared to the sparser Optech data (1.4 points m^{-2}). Table 3 summarizes the leave-one-out cross-validated rRMSEs for the models. A comparison using the point-weighted vegetation ratio (i.e., compensating for uneven distribution of the laser returns) in the models was conducted with results also shown in Table 3.

Table 3. *Leave-one-out cross-validated relative root mean square error. Comparison with and without point-weighted vegetation ratio used in the multiple linear regression.*

	rRMSE with pw[a]		rRMSE without pw[a]	
Variable	TopEye	Optech	TopEye	Optech
Above ground tree biomass	18.7%	21.2%	19.9%	22.1%
Maximum tree height	8.8%	9.5%	8.9%	9.6%
Vertical canopy cover	16.8%	18.7%	19.1%	19.9%

[a] Point-weighted vegetation ratio.

Figure 5a shows a forested sample plot from above illustrating the uneven coverage of points in the helicopter acquisition (TopEye). Figure 5b shows the same sample plot from the more evenly distributed point cloud collected from fixed wing aircraft (Optech). Figure 5c and 5d illustrate the same sample plot, but taken from the side. Figure 6 shows a raster map with predicted values of above ground biomass from the TopEye acquisition. The map is extrapolated outside the area calibrated with sample plots to give an overview of the mosaic patterned forest-tundra ecotone in this area.

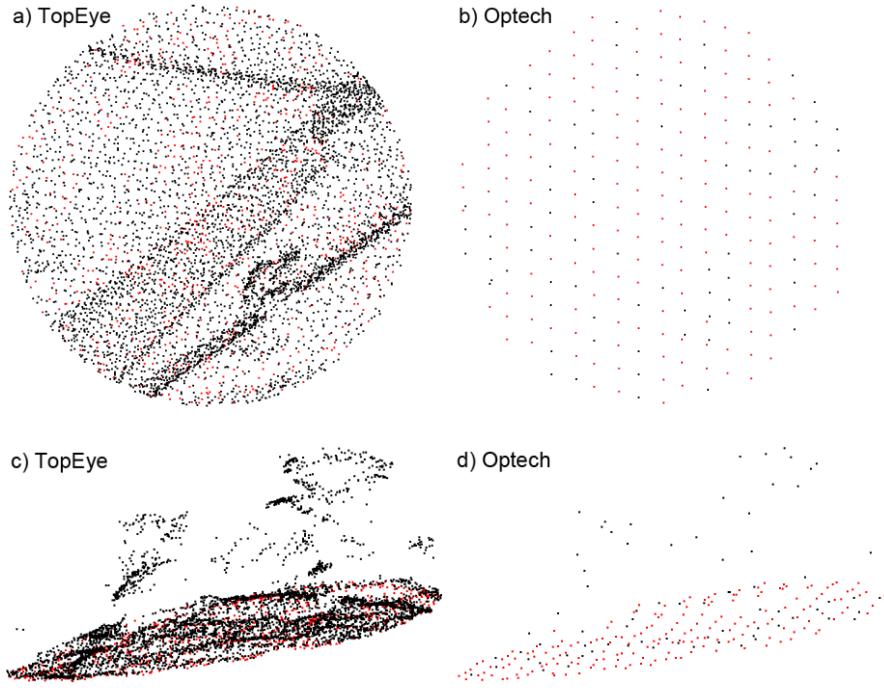

Figure 5. Point cloud of a forested sample plot with 10 m radius. Red points are classified as ground returns and black points are non-ground. View from top in a and b and from side in c and d. Point density for this particular sample plot is 19.7 m^{-2} for TopEye and 0.8 m^{-2} for Optech.

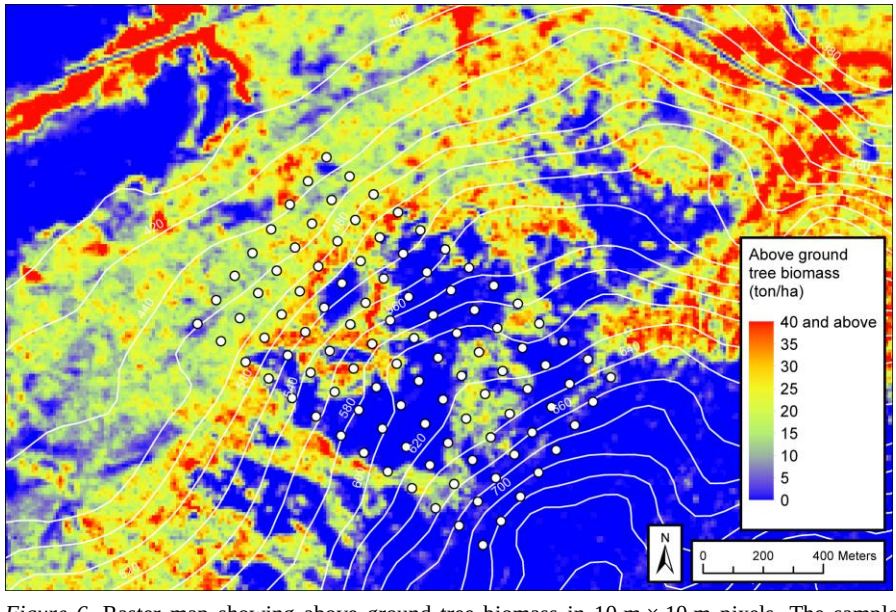

Figure 6. Raster map showing above ground tree biomass in 10 m × 10 m pixels. The sample plots are marked with circles. © Lantmäteriet, i2012/901.

4.2 Combining airborne laser scanning data and optical satellite data for classification of alpine vegetation (paper II)

Laser metrics improved the overall classification accuracy by 5.9 percentage points compared to SPOT 5 satellite data and elevation derivatives (from 57.2% to 63.1%) and by 14.2 percentage points compared to SPOT 5 satellite data alone (48.9%). Alpine willow and mountain birch were the two classes benefitting the most from the addition of laser metrics. Table 4 gives an overview of the producer's and user's accuracy for the vegetation classes. The producer's classification accuracy of mountain birch increased from 55.8% using satellite data alone to 98.1% when adding laser metrics and elevation derivatives to the classification, and from 18.2% to 54.6%, respectively, for alpine willow. The other vegetation classes showed only slightly higher producer's accuracy when laser metrics were included and sometimes decreased accuracy (e.g., grass heath). The user's accuracy increased for most classes when adding laser metrics. The addition of elevation data to the satellite data also increased the accuracy for several classes. When using only laser metrics and elevation, the classification accuracy was much lower for most classes. Figure 7 shows an area of classifications where mountain birch, alpine willow, and mesic heath classification has been influenced when adding laser metrics. The variable selection showed that the following laser metrics were important for the classification and therefore included: H_{95}^{nDSM}, H_{99}^{nDSM}, H_{mean}^{nDSM}, H_{sd}^{nDSM}, H_{sum}^{nDSM}, D_{3}^{nDSM}, $VR_{thresh=0.1}^{CH}$, $VR_{thresh=0.1}^{CH}/VR_{thresh=0.2}^{CH}$, $VR_{\sigma(thresh=i)}^{CH}$, and elevation derivatives: elevation, slope, and the wetness index.

Table 4. *Producer's and user's accuracy (%) by class given the different input data sources.*

Indata	Producer's accuracy				User's accuracy				
Satellite (S)	S	S	S	--	S	S	S	--	Total # reference plots
Elev. deriv. (E)	E	E	--	E	E	E	--	E	
Laser metrics (L)	L	--	--	L	L	--	--	L	
Grass heath	52.9	58.8	58.8	29.4	29.0	28.6	27.0	15.2	17
Ext. dry heath	60.0	50.0	40.0	40.0	40.0	35.7	21.1	25.6	10
Dry heath	75.0	77.5	57.5	40.0	36.6	35.2	30.7	22.2	40
Mesic heath	20.8	13.2	18.9	17.0	47.8	38.9	38.5	39.1	53
Alpine meadow	39.3	39.3	35.7	21.4	34.4	29.7	22.2	15.8	28
Snowbed	51.3	48.7	48.7	53.9	100.0	100.0	100.0	100.0	39
Wetland	60.0	60.0	50.0	42.9	80.0	63.2	71.4	60.0	20
Alpine willow	54.6	40.9	18.2	35.6	75.0	75.0	28.6	32.0	44
Mountain birch	98.1	65.4	55.8	98.1	82.4	72.3	65.9	85.0	52
Bare rock	82.0	76.0	82.0	24.0	95.4	95.0	97.6	44.4	50
Snow	100.0	100.0	100.0	63.0	100.0	100.0	100.0	63.6	11
Water	100.0	100.0	100.0	90.0	100.0	100.0	100.0	75.0	10

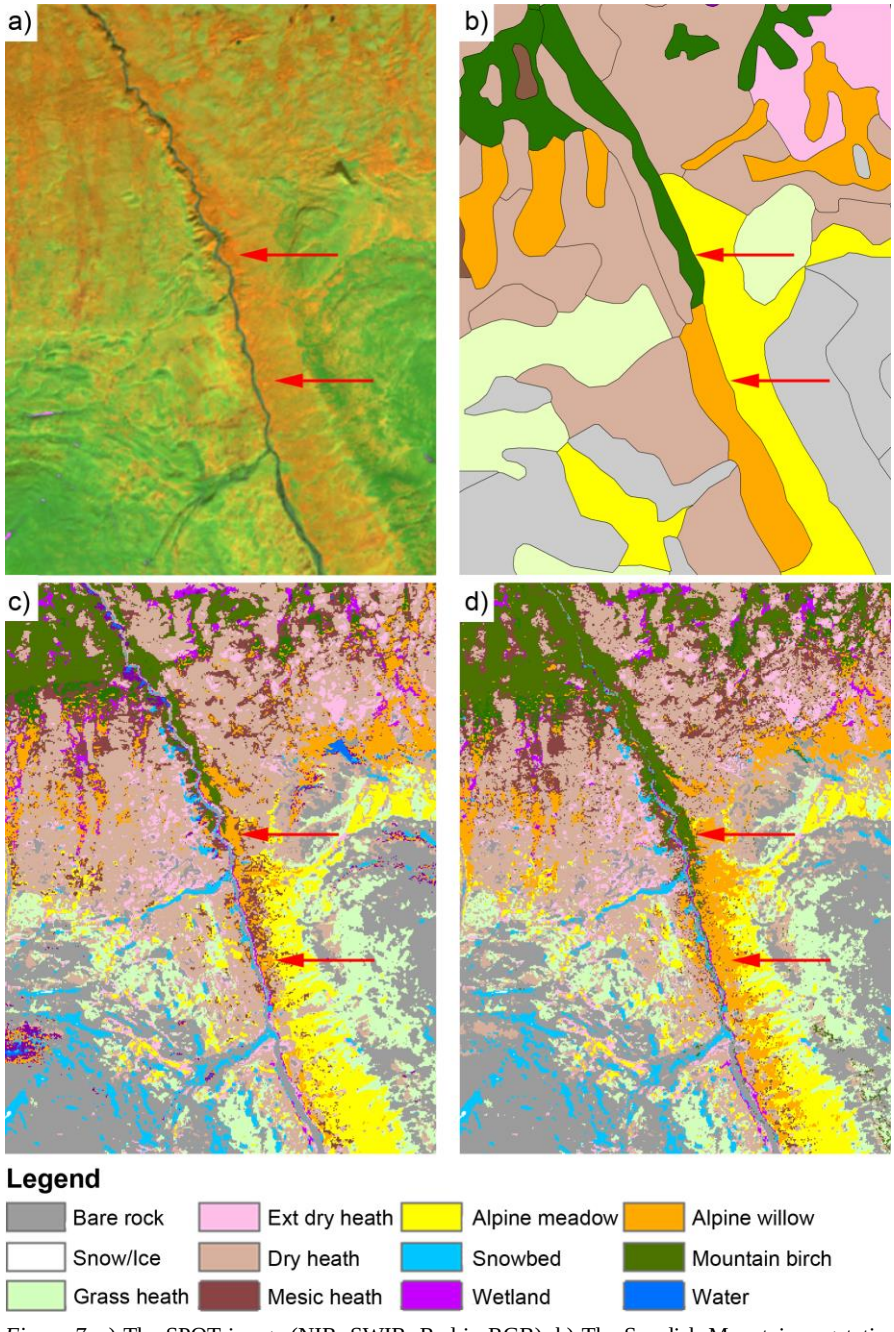

Figure 7. a) The SPOT image (NIR, SWIR, Red in RGB); b) The Swedish Mountain vegetation map; c) Classification from SPOT + elevation derivatives; d) Classification of SPOT + elevation derivatives + laser metrics. The uppermost red arrow shows where laser data improved separation between mountain birch and willow and the lower red arrow shows improved separation between willow and mesic heath. © Lantmäteriet, i2012/901.

4.3 Change detection of mountain birch using multi-temporal ALS point clouds (paper III)

The laser metrics from the Optech scanning were histogram matched to the histograms of laser metrics from the TopEye scanning. Figure 8 shows examples of cumulative histograms for two of the laser metrics used in paper I: the normalized sum of squared heights (H_{sum}^{CH}) and the point-weighted vegetation ratio of first returns ($VR_{pw,1st}^{CH}$). Figure 9 shows one-to-one plots of the same two laser metrics without calibration and calibrated using histogram matching. In the figure it can be seen that after histogram matching was applied, the relationship between the metrics from the two sensors is no longer curved.

The similarity of the laser metrics between the two acquisitions were evaluated by calculating rRMSE and rBias for the reference sample plots. Table 5 shows the similarity of the laser metrics used in paper I. In general, laser metrics calculated from nDSM tend to have lower rRMSE and rBias than metrics calculated using CH. The rBias always has a low value when histogram matching is used.

When classifying the sample plots into the three experimental classes, the laser metrics based on the density of the vegetation resulted in general in higher classification accuracy (overall classification accuracy 87.5%) than the laser metrics based on the height of the vegetation (overall classification accuracy 81.3%). Slightly higher classification accuracy (88.5%) was achieved when the best combination of two laser metrics was used, namely height density 1 (D_1^{nDSM}) and the 95th height percentile (H_{95}^{CH}). When using only a height percentile, almost none of the sample plots from the 50% changed class were correctly classified. Considerably higher classification accuracy for the 50% changed class was achieved when using a measure of density (e.g., D_1^{nDSM}).

Table 5. *rRMSE (%) and rBias (%) for the laser metrics used in paper I calculated for the 68 reference sample plots.*

Laser metric	rRMSE Uncalibrated	rRMSE Histogram matched	rBias Uncalibrated	rBias Histogram matched
H_{95}^{CH}	8.5	6.7	4.5	-0.2
H_{sum}^{CH}	13.6	13.7	-0.6	-1.6
$VR_{pw,1st}^{CH}$	23.4	16.5	12.0	-2.4
$VR_{pw,all}^{CH}$	18.1	16.4	-1.2	-1.8

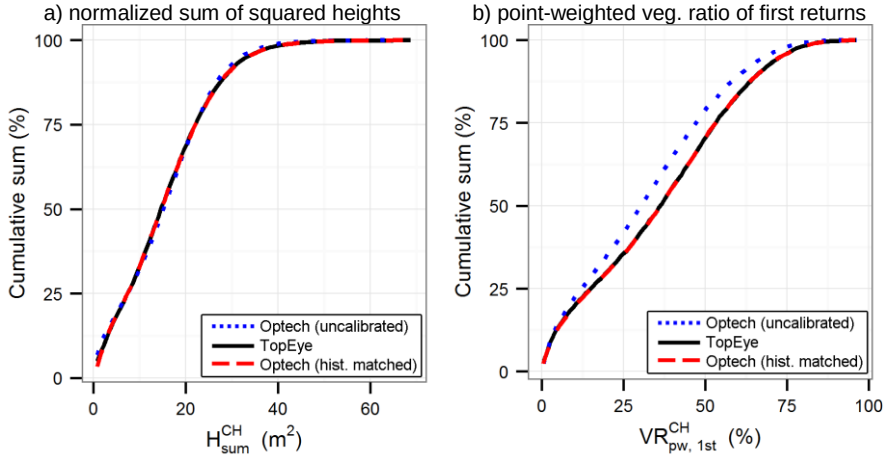

Figure 8. Cumulative histograms of two metrics also used in paper I.

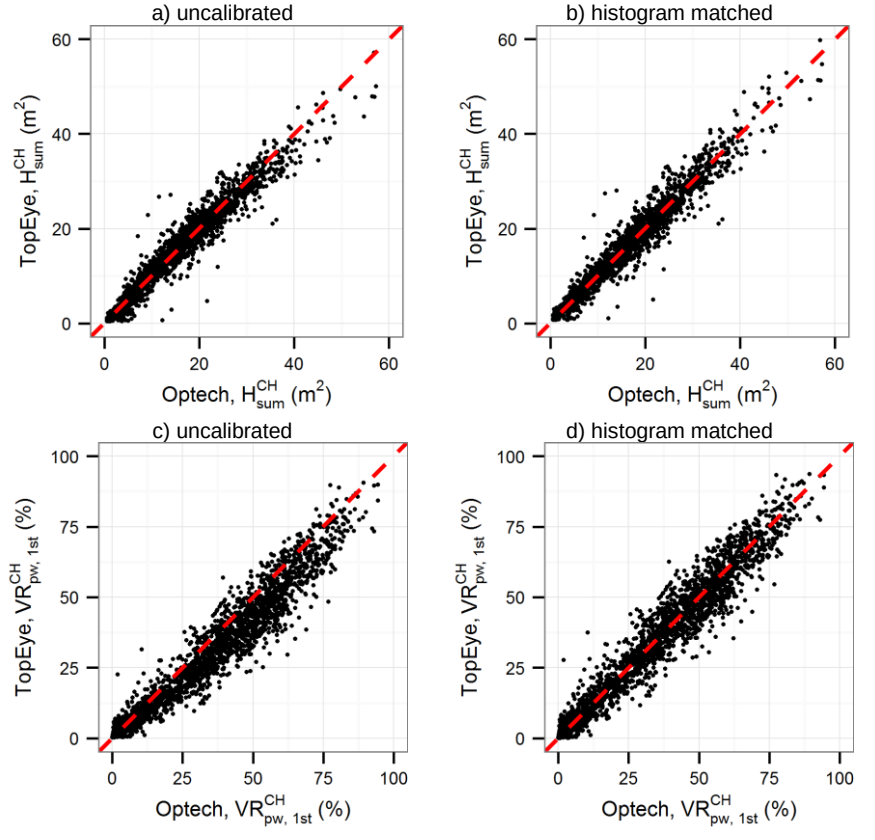

Figure 9. One-to-one plot before and after applying histogram matching. The dashed line is the one-to-one line. Only every fifth point is plotted. a, b) normalized sum of squared heights (H^{CH}_{sum}), c, d) point-weighted vegetation ratio of first returns ($VR^{CH}_{pw,1st}$).

4.4 Detecting afforestation at individual tree level using ALS (paper IV)

The height of the 0.3 m to 2.6 m tall trees could be measured with high precision at the first scanning occasion (standard deviation = 0.3 m), however, there was a systematic underestimation (Figure 10a). It could also be seen that the height of some individuals were clearly overestimated, most likely due to the presence of nearby taller trees. The mean difference and standard deviation of the difference between laser measured and field measured tree heights was -0.15 m and 0.32 m, respectively.

Figure 10b shows a positive correlation for the field measured height change and the difference between the two nDSMs. The 1-1 line in Figure 10b translated to the 100% removed trees (crosses) shows that there was a systematic shift and that height changes for trees with a small initial height are not measurable.

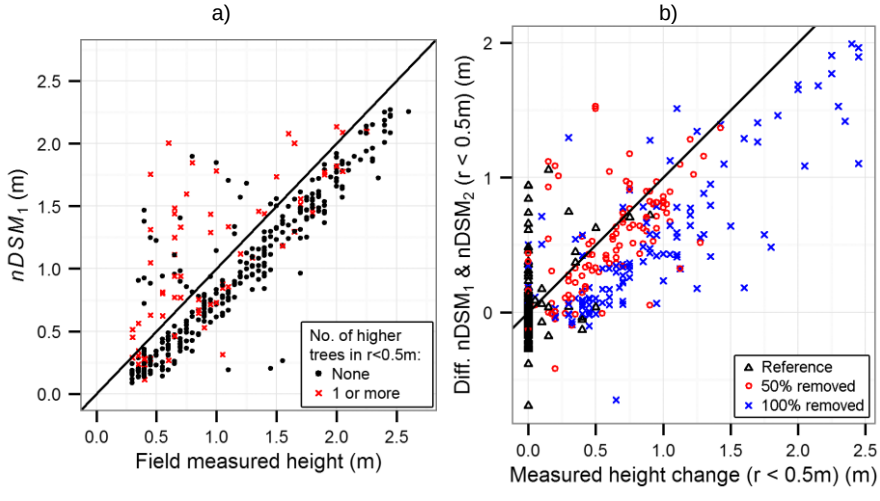

Figure 10. Black line is 1-1. a) Field measured height at the first scanning plotted against laser derived height, i.e., maximum $nDSM_1$ height within 0.3 m radius from the field coordinate. Different symbols are used to show that most of the trees with overestimated heights have a taller tree within a 0.5 m radius. b) Field measured height change within 0.5 m radius from the field coordinate versus difference between maximum height in $nDSM_1$ and $nDSM_2$ within 0.5 m radius from the field coordinate.

LDA classification was performed using $nDSM_1$ and $nDSM_2$ heights within a 0.3 m radius around the field coordinates as discriminators. Leave-one-out cross-validated overall accuracy for the three classes (i.e., reference, 50% removal, 100% removal) was 63%. When only trees taller than 1 m were included, the overall accuracy increased to 75%. When aggregating the 50%

removal and 100% removal classes, the corresponding overall accuracy was 88% for trees taller than 1 m. Table 6 shows an error matrix for all trees taller than 1 m where the 50% and 100% change classes have been aggregated.

Table 6. *Error matrix for linear discriminant analysis classification of all trees ≥ 1 m height into the classes reference and an aggregated change class with 50% or 100% of the trees removed.*

	Field data		
Predicted	Reference	50+100% removed	User's accuracy
Reference	70	17	80.5%
50+100% removed	7	108	93.9%
Producer´s accuracy	90.9%	86.4%	Overall: 88.1%

4.5 Detection of windthrown trees using airborne laser scanning (paper V)

Windthrown trees were discriminated using a difference elevation model (OHM) between a smooth model of the ground and a more elastic model created using an active surface (Figure 11a). Windthrown trees can clearly be seen in the OHM, but also other rough objects close to the ground are present, for example bushes, ditches, and boulders.

Template matching was used to automatically detect windthrown trees in the OHM (Figure 11b). In the 54 ha study area, 2,628 objects were detected as potentially being windthrown trees. LDA classification reduced the number of objects to 480 using training data. Of the total 651 windthrown trees in the study area, 247 were automatically linked to trees detected by template matching in the OHM. The number of detected trees that could not be linked to a field measured windthrown tree was 233, which corresponds to a commission error rate of 36%. Figure 11b gives an overview of detection, commission and omission of windthrown trees in a close-up within the study area. It can be noted that some true windthrown trees from the automatic detection were not linked to the field measured windthrown trees because they did not fulfill the linking criteria (distance and angle).

In Figure 12, trends can be seen in the probability of detecting a windthrown tree based on field measured tree length and density of the remaining forest within a 12 m radius around the field measured coordinate of the windthrown tree. When aggregating the results to 40 m square grid cells, at least one tree was detected in 77% of the grid cells that included windthrown trees and 34% of the grid cells without windthrown trees were falsely detected as having windthrown trees.

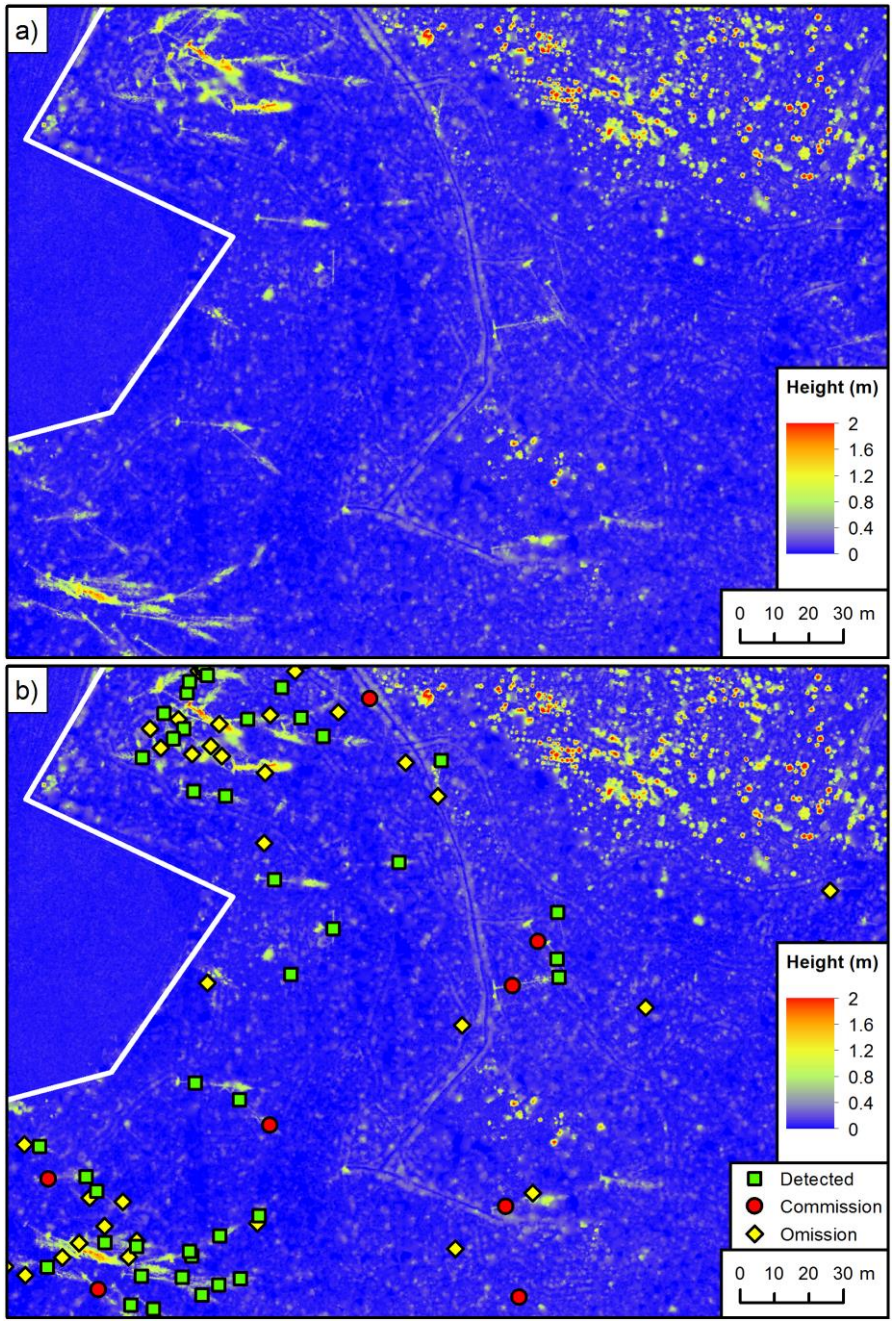

Figure 11. a) A close-up within the study area to illustrate the object height model (OHM). The OHM is created by subtracting the ground DEM from the active surface DEM. b) OHM with the results from the detection of windthrown trees. Note that the field measured coordinates can have a positional error of several meters. The white border is the extent of the study area.

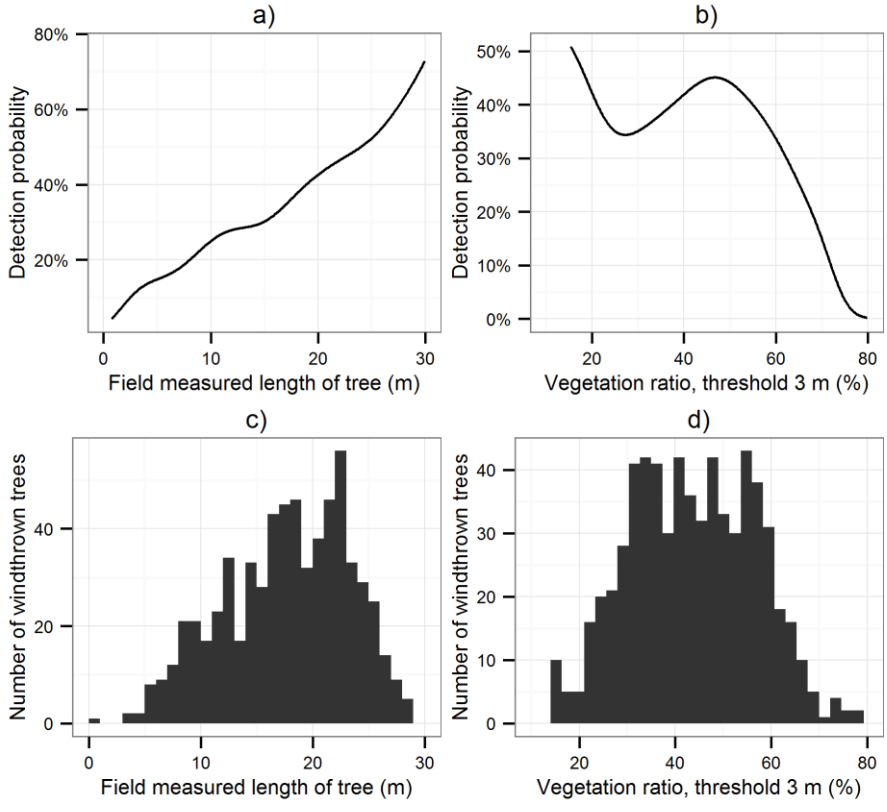

Figure 12. Probability of detecting a windthrown tree based on a) field measured length of the windthrown tree and b) the crown coverage represented as vegetation ratio within a 12 m radius. c, d) Histograms of total number of windthrown trees. Note that there are few observations in the lower and upper limits.

5 Discussion

5.1 The forest-tundra ecotone

Paper I shows that maximum tree height, above ground tree biomass, and vertical canopy cover for sub-arctic mountain birch forest can be predicted with high precision using ALS data. To my knowledge, this is the first time ALS-based biomass predictions for this type of forest have been reported, since earlier ALS studies of mountain birch concentrated on the existence of forested areas (e.g., Rees, 2007; Ørka *et al.*, 2012), and the existence of pioneer trees (e.g., Næsset & Nelson, 2007; Næsset, 2009b; Thieme *et al.*, 2011; Stumberg *et al.*, 2012). Three studies have been found which were carried out in mountain environments with steep inclination, but in areas containing much taller trees and dominated by spruce: Hollaus *et al.* (2007, 2009) and Jochem *et al.* (2011) predicted stem volume and above ground biomass for Austrian mountain forest.

A new method to weight unevenly distributed laser returns in relation to the density of surrounding points was presented in paper I. The combination of a heterogeneous forest canopy and an uneven distribution of laser points within the sample plot might cause unrepresentative relationships between laser metrics and forest data. The solution presented in paper I weights each point based on the density of surrounding points within a given radius when calculating the vegetation ratio. Visual inspection revealed that TopEye laser data points were more unevenly distributed than in the Optech data (e.g., Figure 5). This was most likely the reason why the point weight correction had a larger improvement on the TopEye data. An advantage with the method is that the point cloud does not need to be decimated, which is the case for the gridding method presented by Vauhkonen *et al.* (2008).

The foot-print was about 0.5 m with both laser scanners regardless of the difference in flying altitude. This causes the Optech scanner with low point density to omit some vegetation because the ground is not fully illuminated. In

paper I the predictions using the Optech were good in any case because all sample plots which had a few trees also had at least a few points from the vegetation. The results in paper II could probably have been improved with higher point density ALS data, especially for some of the vegetation classes such as mesic heath. In paper III it was found that plots with few trees were more difficult to classify if they had changed or not than plots with many trees. A probable reason is that sample plots with few small trees (tree height <3.5 m) had too few hits in the vegetation in the sparse second scanning causing inaccurate laser metrics.

In paper II, a problem was noticed using the $VR^{CH}_{thresh=0.1}$ metric as it was often equal to zero because there were no hits higher than 0.1 m above the ground DEM. The previously mentioned problem with low point density could be a reason for this. The use of full waveform data could probably increase the accuracy for the classes with low vegetation (<1 m). Full waveform data can give more information about returns, for example pulse-width.

5.2 Change detection

It has been shown in previous studies, such as Yu *et al.* (2005) that two ALS datasets collected with different scanners could result in bias in height growth estimates. It is of interest to further analyze differences between instruments and how to make acquisitions from different sensors comparable and measurable. Paper III suggests the use of histogram matching of the laser metrics from two acquisitions. With this method, changes cannot be measured in absolute numbers, but rather as relative to the normal growth of the vegetation in the area used as reference for the histogram matching algorithm.

As noticed by Næsset & Gobakken (2005), the 100th height percentile is less suitable for multi-temporal use, because it tends to be less stable. Paper III showed the same result, as the 100th height percentile (H^{nDSM}_{100}) had a rRMSE of 11.9% and the 95th height percentile (H^{nDSM}_{95}) a rRMSE of 9.2%. This showed that the 95th height percentile was more similar between the two acquisitions than the 100th height percentile. A reason why the 100th height percentile tends to be less stable is that it is based only on the single highest return. Hudak *et al.* (2012) found that there was more underestimation of tree height with sparse pulse density ALS compared to dense when using the maximum canopy height from ALS. Hudak *et al.* also noticed that mean canopy height from ALS was less subject to such bias.

In paper III, rRMSE and rBias (Table 5) were calculated using the 68 reference sample plots without experimental changes to evaluate similarity between the two datasets. The height percentiles appeared to be more similar

than the density metrics due to the lower rRMSE noticed. Bater *et al*. (2011) compared four acquisitions from the same day and also noted that the height percentiles were more stable than density metrics. A possible reason is that the height percentiles are less sensitive for view angle effects (Holmgren *et al.*, 2003).

The laser metrics created using nDSM values have lower rRMSE for the reference plots and provide higher classification accuracy than metrics created from CH. Multi-temporal data requires measures to be spatially normalized at each acquisition to avoid problems with uneven distribution of laser points (paper I).

Many other studies compare multi-temporal data for shift in elevation, but in papers I, III and IV in this thesis, this was not done as a ground DEM was created from each dataset. The horizontal errors will probably have minor effect on the results in paper III, but could have a quite large effect on the results in paper IV. In paper IV a visual analysis of a few trees was performed to check for horizontal shifts, but only minor shifts could be seen and could have been caused by the wind.

5.3 Remote sensing of afforestation

Paper IV demonstrated how the height of individual trees in the height range 0.3 m to 2.6 m could be measured with high precision despite a large amount of surrounding grass with the same heights as the smaller trees (0.3–1 m tall). This is the first known study where removal of small trees (≤2.6 m tall) have been detected on individual tree level using ALS data from two time points. However, in Thieme *et al.* (2011) small trees were detected in the mountains using data from a single time point and the results were evaluated in a similar way as in paper IV using a radius around field measured tree positions. In that study, the proportion of detected trees was 90%, which is comparable to the 88% overall classification accuracy for trees taller than 1 m in paper IV. However, in Thieme *et al*. the detection rate for trees shorter than 1 m was only 49%, as compared to 72% in paper IV. Hellesen & Matikainen (2013) used a combination of ALS and ortho-photos from one time point of grasslands in Denmark to classify vegetation. They created segments that were classified in three classes including a class with shrubs and trees and obtained a producer's accuracy of 93.7%.

ALS data from two time points were used in paper IV which provides the advantage that non-changed objects, such as large stones, can be eliminated from the analysis. In paper V, ALS data were used from only one acquisition

and the non-changed objects will then cause some false detections of windthrown trees (e.g., young forest is included in the OHM in Figure 11a).

It is important to co-register the two acquisitions if the ground DEM is not created from each acquisition as in paper III and IV. Most of the previous studies have done co-registration by systematically adjusting the height based on returns from a hard surface or using field measured control points. In paper IV, the DEM from the first scanning had a mean offset of 0.12 m above the true ground and the DEM from the second scanning had a mean offset of 0.10 m above the true ground. The comparison was done with the field measured elevation for all field trees (383 measurements). As the mean offset was 0.15 m (Figure 10a), the height underestimation measured at the first acquisition is less than one decimeter if the DEM would have been aligned to the true ground. The influence of low vegetation on the ALS point cloud has been undertaken in several studies, including Ahokas *et al.* (2003) and Pfeifer *et al.* (2004). For both of these studies, the conclusion is the same; the laser measurements are higher than the field measured control points, especially when vegetation is present.

Analysis of the horizontal mismatch between the two acquisitions in paper IV has not been undertaken. The height change from the ALS data (Figure 10b) is less correlated to the field measured height change than compared to the use of absolute measurements from the first date ALS dataset (Figure 10a). Some possible reasons are geometrical mismatch between the two nDSMs, influence of wind on the exact position of the small tree crowns, and influence from nearby trees or other vegetation within the selected radius (0.5 m). A future improvement could be to use unchanged objects to check and correct for horizontal displacements between multiple acquisitions or by tree-to-tree matching (Yu *et al.*, 2008).

5.4 Detection of windthrown trees

In paper V, a new method to detect windthrown trees was developed and evaluated. The method uses an OHM derived from the difference between two height models created from the same laser dataset, where the first is a model of the ground elevation and the second is an elastic surface of the ground elevation that also includes objects near the ground (e.g., stones, downed trees, etc.). This approach was successful in making use of the laser beam's penetration through the vegetation layer to reach objects near ground level. An automatic tree detection method was developed based on the OHM, but manual interpretation of the OHM could also be done. By visual inspection, the results obtained from the OHM were judged to be as good as those from low altitude

aerial photos for identifying windthrown trees in open areas. However, from the OHM, windthrown trees could also be identified in closed forest (paper V).

The template matching method used to automatically detect windthrown trees in the OHM was found to be useful, but a large amount of commission errors were produced if used without a training phase. The commission errors occurred because many other objects near the ground had shapes similar to windthrown trees, for example, road, edges of ditches, shrubs in a line, etc. One way could be to use methods to locate longer linear structures to reduce problems with these objects (e.g., Rutzinger *et al.* (2011) where roads were extracted from ALS data). In paper V, field data were used to classify falsely detected trees in order to reduce the commission errors. In a future operational case, this step would still be necessary, but instead of collecting field data, an interpreter could identify windthrown trees in the OHM and in that way create training data for the classification of falsely detected trees. In Blanchard *et al.* (2011), the ground truth data were created by visually identifying windthrown trees in aerial photos and ALS data. This could cause an underestimation as some trees might be occluded or missed. In the study by Lindberg *et al.* (2013) a large amount of commission errors were also obtained. They detected 41% of 651 downed logs, but had a commission error rate of 89%, compared to detecting 38% of the logs and commission error rate of 36% in paper V.

The results of the detection in paper V were analyzed to find characteristics of terrain and windthrown trees needed for successful detection. Figure 12a shows an analysis of the probability of detecting a windthrown tree given the field measured tree length. There is a clear trend where shorter trees have much lower probability of detection compared to the longer trees. An analysis was also performed on the density of the remaining forest within a 12 m radius around the field measured coordinate of the windthrown tree (Figure 12b). The result is quite clear also for this figure: the higher the forest density, the lower the probability of detecting a windthrown tree on the ground. It should be noted though that the number of observations are few in the lower and upper limits (Figure 12c and d).

In the study by Mücke *et al.* (2013) the downed trees had much larger DBH than in paper V. Mücke *et al.* used full waveform ALS data and detected 76% of the 82 field surveyed trees in the area and had a low commission rate of 9%. The results in paper V could have been improved by using a scanner with a lower scan angle or waveform data to extract as many points as possible near the ground and to make use of the echo width as in Mücke *et al.* (2013).

Blanchard *et al.* (2011) used object-based image analysis to detect downed logs using ALS data. They collected the ground truth data by interpreting downed trees in aerial photos and ALS data, which might cause higher

detection rate as some of the downed trees might be missed. Blanchard *et al.* completely or partially detected 73% of 103 downed logs. They also noticed that over-classification occurred in areas where a large number of logs were clustered and in areas with shrub and tree canopies, but no commission error numbers were presented. The method used in paper V was successful in detecting trees in closed forest but resulted in under-classification in areas where a large number of logs were clustered. As seen in Figure 12b, the detection probability was about the same for vegetation ratios up to 60% of the surrounding forest.

It can also be seen in Figure 11b that some true windthrown trees have been identified as commission errors because they have not been automatically linked to a field measured windthrown tree. The reasons for this can be that the horizontal location of the field measured trees was measured with a GPS which produced errors of several meters. This could have been solved by increasing the search radius when linking, but that could also cause false links.

5.5 Conclusions

The following summarizes the main findings in this thesis:

- The area based method was used to predict maximum tree height, above ground tree biomass, and vertical canopy cover with high precision in the forest-tundra ecotone using ALS data. Low (1.4 points m^{-2}) and high density (6.1 points m^{-2}) ALS data were compared for predictions of the three variables. Despite the big difference in point density, the low density data produced only slightly worse results (e.g., relative RMSE of biomass 21.2% vs. 18.7%).
- A new algorithm to correct for uneven distribution of laser returns, without decimating the data, was developed. The method especially improved predictions of variables strongly related to forest density. The prediction of vertical canopy cover from helicopter acquired ALS data had improved relative RMSE from 19.1% to 16.8% when the new algorithm was used.
- When adding laser metrics from ALS data and elevation derivatives to the classification of mountain vegetation, a considerable classification improvement was seen for mountain birch forest and alpine willow. Compared to using only optical satellite data, the classification accuracy improved from 56% to 98% for mountain birch and from 18% to 55% for alpine willow.

- Histogram matching was proven to be efficient for calibration of laser metrics from two ALS acquisitions to locate local changes that differ from the normal development of the landscape.
- When comparing laser metrics from two ALS acquisitions over the same area, laser metrics calculated using nDSM tended to be more stable than metrics calculated using CHs.
- Establishment of small trees (0.3–2.6 m tall) in agricultural grassland can be found with high accuracy when they are at least of the same height as the surrounding grass (>1 m above ground). The overall accuracy when classifying trees as changed and unchanged was 88% for 202 field measured trees taller than 1 m.
- A difference between a smooth and a flexible elevation model from ALS data reveals objects close to the ground including windthrown trees. By using template matching, the windthrown trees could automatically be located. At individual tree level, 38% of the windthrown trees were successfully linked to the 651 field measured trees. When aggregating to 40 m grid cells, at least one tree was found in 77% of the cells that included windthrown trees.
- It was found that larger windthrown trees had a higher detection rate than shorter trees when using template matching to automatically locate windthrown trees.

5.6 Future work

5.6.1 Reproducibility of measurements

One aim of this thesis was to develop methods for future utilization of time-series of 3D measurements of vegetation obtained from ALS. One important task was therefore to find stable laser metrics that were insensitive to system parameter settings and external factors during the data acquisition. In paper I and paper III, the uneven distribution of ALS points led to unrepresentative metrics. Paper I came up with a solution to this: weighting the points based on the density of surrounding points. The drawback with this method is that a radius needs to be set which is dependent on the density of the data. A solution where no settings are needed is of interest.

For change detection it is of interest to investigate how the returns are extracted in the different acquisitions. Full waveform data collected over the same area could result in more stable metrics if the same method were to be used to extract the returns from the acquisitions, but will however not solve the problem with false changes due to different phenology at the two acquisitions.

5.6.2 Area based classification and change detection

Sparse density ALS data were used in paper II. There were considerable improvements for the two taller vegetation classes (>0.5 m), namely mountain birch and alpine willow. Future research should consider higher density ALS data and full waveform, which probably could also improve some of the lower-growing vegetation classes.

Repeated monitoring of changes in the forest-tundra ecotone using ALS data will probably be costly. One option is to use 3D point clouds computed by matching aerial photos which are collected every fifth year for the Swedish mountain region. By using the DEM representing ground from ALS data, vegetation heights can be calculated from the photogrammetric point cloud. The results are relatively good for height of the vegetation, but density measures are difficult because of the difficulties to match the ground under the tree canopies (White *et al.*, 2013). ALS is an active source and penetrates the vegetation resulting in a good measure of vegetation density. Two options for future monitoring of the forest-tundra ecotone are suggested: repeated ALS scans of strips or by initially covering the whole area with ALS data to achieve a high resolution ground DEM and then repeated collection of aerial photos for creation of 3D point clouds using matching. Further research should be done to assess the best option to set up a monitoring system for the forest-tundra ecotone.

5.6.3 Object based classification and change detection

In paper IV, no automatic detection of trees was used, but this would be the next step in future research as well as evaluation of the effect of, for example, flight direction and scan angle.

In paper V it was shown that features close to the ground, such as newly windthrown trees, could be detected using data from only one time point. There were some problems with boulders, roads, ditches, and bushes causing false identifications as windthrown trees. By also using data collected before the storm, the false identifications should be the same and errors would most likely be reduced by using a difference image.

The high density data used in paper IV and V are currently expensive and take a longer time to collect than sparse data. Photon counting ALS will be a future option that creates point densities similar to the ones used in paper IV and V flown at a much higher flying altitude and thereby at a lower cost (Harding *et al.*, 2011; Rosette *et al.*, 2011).

After storms it is not always easy to order an ALS acquisition on short notice. An unmanned aerial vehicle (UAV) carrying a laser sensor would

therefore be an option. It is shown to be technically possible by Lin *et al.* (2011) and Wallace *et al.* (2012).

The use of sampling should be further investigated for the purpose of estimating total numbers of windthrown trees after storms. One option could be to use two-phase sampling with ALS strips and a limited number of field surveyed areas.

After four years of reading and writing about ALS data use for vegetation purposes, I have found that most studies use an empirical approach. I hope that more studies in the future will also investigate physical approaches to the problems. A reason for the empirical approach is probably the limited information delivered with airborne laser scanning data. Close cooperation with the manufacturer of the scanner is probably needed to access the necessary information for studying physical properties of the data.

References

ACIA (2004). *Arctic climate impact assessment*. Cambridge, UK.

Ahokas, E., Kaartinen, H. & Hyyppä, J. (2003). A quality assessment of airborne laser scanner data. In: Proceedings of ISPRS Archives – Vol. XXXIV-3/W13, Dresden, Germany, October 8-10, 2003.

Allen, T. R. & Walsh, S. J. (1996). Spatial and compositional pattern of alpine treeline, Glacier National Park, Montana. *Photogrammetric Engineering and Remote Sensing* 62(11), 1261–1268.

Aune, S., Hofgaard, A. & Söderström, L. (2011). Contrasting climate- and land-use-driven tree encroachment patterns of subarctic tundra in northern Norway and the Kola Peninsula. *Canadian Journal of Forest Research* 41(3), 437–449.

Axelsson, P. (1999). Processing of laser scanner data - algorithms and applications. *ISPRS Journal of Photogrammetry & Remote Sensing* 54(2-3), 138–147.

Axelsson, P. (2000). DEM generation from laser scanner data using adaptive TIN models. *International Archives of Photogrammetry & Remote Sensing* 33, 110–117.

Balzter, H., Skinner, L., Luckman, A. & Brooke, R. (2003). Estimation of tree growth in a conifer plantation over nineteen years from multi-satellite L-band SAR. *Remote Sensing of Environment* 84, 184–191.

Bater, C. W., Wulder, M. A., Coops, N. C., Nelson, R. F., Hilker, T. & Næsset, E. (2011). Stability of sample-based scanning-LiDAR-derived vegetation metrics for forest monitoring. *Geoscience and Remote Sensing, IEEE Transactions on* 49(6), 2385–2392.

Bebber, D. & Thomas, S. (2003). Prism sweeps for coarse woody debris. *Canadian Journal of Forest Research* 33, 1737–1743.

Blanchard, S. D., Jakubowski, M. K. & Kelly, M. (2011). Object-based image analysis of downed logs in disturbed forested landscapes using lidar. *Remote Sensing* 3(11), 2420–2439.

Van Bogaert, R. (2010). *Recent treeline dynamics in sub-arctic Sweden: a multi-disciplinary landscape assessment*. Diss. Universiteit Gent. Available from: https://biblio.ugent.be/publication/3033327. [Accessed 2012-12-07].

Van Bogaert, R., Haneca, K., Hoogesteger, J., Jonasson, C., De Dapper, M. & Callaghan, T. V. (2011). A century of tree line changes in sub-Arctic Sweden shows local and regional variability and only a minor influence of 20th century climate warming. *Journal of Biogeography* 38(5), 907–921.

Bollandsås, O. M., Gregoire, T. G., Næsset, E. & Øyen, B.-H. (2013). Detection of biomass change in a Norwegian mountain forest area using small footprint airborne laser scanner data. *Statistical Methods & Applications* 22(1), 113–129.

Bouget, C. & Duelli, P. (2004). The effects of windthrow on forest insect communities: a literature review. *Biological Conservation* 118(3), 281–299.

Brandtberg, T. (1999). *Automatic individual tree-based analysis of high spatial resolution remotely sensed data*. Diss. Swedish University of Agricultural Sciences.

Breiman, L. (2001). Random forests. *Machine Learning* 45, 5–32.

Böhner, J., Köthe, R., Conrad, O., Gross, J., Ringeler, A. & Selige, T. (2002). *Soil regionalisation by means of terrain analysis and process parameterisation*. European Soil Bureau. Available from: http://www.scilands.de/referenzen/veroeffentlichung/601Bohner.pdf. [Accessed 2013-11-29].

Callaghan, T. V, Werkman, B. R. & Crawford, R. M. M. (2002). The tundra-taiga interface and its dynamics: Concepts and applications. *Ambio* 12, 6–14.

Clements, F. E. (1936). Nature and structure of the climax. *The Journal of Ecology* 24(1), 252–284.

Congalton, R. G. (1991). A review of assessing the accuracy of classifications of remotely sensed data. *Remote Sensing of Environment* 37(1), 35–46.

Coops, N. C., Morsdorf, F., Schaepman, M. E. & Zimmermann, N. E. (2013). Characterization of an alpine tree line using airborne LiDAR data and physiological modeling. *Global change biology* 19(12), 3808–3821.

Coppin, P., Jonckheere, I., Nackaerts, K., Muys, B. & Lambin, E. (2004). Digital change detection methods in ecosystem monitoring: a review. *International Journal of Remote Sensing* 25(9), 1565–1596.

Dahlberg, U., Berge, T. W., Petersson, H. & Vencatasawmy, C. P. (2004). Modelling biomass and leaf area index in a sub-arctic Scandinavian mountain area. *Scandinavian Journal of Forest Research* 19(1), 60–71.

Day, D. A., Logsdon, J. M. & Latell, B. (Eds.) (1998). *Eye in the sky: The story of the Corona spy satellites*. p 303 Washington, D.C.: Smithsonian Institution Press. ISBN 978-1560988304.

Diaz-Uriarte, R. (2010). varSelRF: Variable selection using random forests. Available from: http://cran.r-project.org/package=varSelRF.

Disney, M. I., Kalogirou, V., Lewis, P., Prieto-Blanco, a., Hancock, S. & Pfeifer, M. (2010). Simulating the impact of discrete-return lidar system and survey characteristics over young conifer and broadleaf forests. *Remote Sensing of Environment* 114(7), 1546–1560 Elsevier Inc.

Donoghue, D. N. M., Watt, P. J., Cox, N. J., Dunford, R. W., Wilson, J., Stables, S. & Smith, S. (2004). An evaluation of the use of satellite data for monitoring early development of young Sitka spruce plantation forest growth. *Forestry* 77(5), 383–396.

Edenius, L., Vencatasawmy, C. P., Sandström, P. & Dahlberg, U. (2003). Combining satellite imagery and ancillary data to map snowbed vegetation important to reindeer Rangifer tarandus. *Arctic, Antarctic, and Alpine Research* 35(2), 150–157.

Elmqvist, M. (2000). *Automatic ground modelling using laser radar data*. Master thesis. Linköping University. Available from: http://www.control.isy.liu.se/student/exjobb/xfiles/3061.pdf. [Accessed 2012-12-22].

Elmqvist, M. (2002). Ground surface estimation from airborne laser scanner data using active shape models. In: Proceedings of ISPRS Archives – Vol. XXXIV, part 3A, Graz, Austria, September 9-13, 2002.

Elmqvist, M., Jungert, E., Lantz, F., Persson, Å. & Söderman, U. (2001). Terrain modelling and analysis using laser scanner data. In: Proceedings of ISPRS Archives – Vol. XXXIV-3/W4, Annapolis, Maryland, USA, October 22-24, 2001.

Estornell, J., Ruiz, L. A., Velázquez-Martí, B. & Hermosilla, T. (2012a). Assessment of factors affecting shrub volume estimations using airborne discrete-return LiDAR data in Mediterranean areas. *Journal of Applied Remote Sensing* 6, 063544.

Estornell, J., Ruiz, L. a., Velázquez-Martí, B. & Hermosilla, T. (2012b). Estimation of biomass and volume of shrub vegetation using LiDAR and spectral data in a Mediterranean environment. *Biomass and Bioenergy* 46, 710–721.

FAO (2004). *Global forest resources assessment update 2005 - Terms and definitions*. Rome, Italy.

Fransson, J. E. S., Walter, F., Blennow, K., Gustavsson, A. & Ulander, L. M. H. (2002). Detection of storm-damaged forested areas using airborne CARABAS-II VHF SAR image data. *IEEE Transactions on Geoscience and Remote Sensing* 40(10), 2170–2175.

Fridman, J. & Walheim, M. (2000). Amount, structure, and dynamics of dead wood on managed forestland in Sweden. *Forest Ecology and Management* 131, 23–36.

GOFC-GOLD (2012). *A sourcebook of methods and procedures for monitoring and reporting anthropogenic greenhouse gas emissions and removals associated with deforestation, gains and losses of carbon stocks in forests remaining forests, and forestation.* GOFC-GOLD Report version COP18-1, (GOFC-GOLD Land Cover Project Office, Wageningen University, The Netherlands.

Goodwin, N. R., Coops, N. C. & Culvenor, D. S. (2006). Assessment of forest structure with airborne LiDAR and the effects of platform altitude. *Remote Sensing of Environment* 103(2), 140–152.

Gove, J. H., Ringvall, A., Ståhl, G. & Ducey, M. J. (1999). Point relascope sampling of downed coarse woody debris. *Canadian Journal of Forest Research* 29(11), 1718–1726.

Gove, J. H., Williams, M. S., Ståhl, G. & Ducey, M. J. (2005). Critical point relascope sampling for unbiased volume estimation of downed coarse woody debris. *Forestry* 78(4), 417–431.

Harding, D. J., Dabneya, P. W. & Valett, S. (2011). Polarimetric, two-color, photon-counting laser altimeter measurements of forest canopy structure. In: Proceedings of International Symposium on Lidar and Radar Mapping 2011, Nanjing, China, May 26-29, 2011.

Hedenås, H., Olsson, H., Jonasson, C., Bergstedt, J., Dahlberg, U. & Callaghan, T. V. (2011). Changes in Tree Growth, Biomass and Vegetation Over a 13-Year Period in the Swedish Sub-Arctic. *Ambio* 40(6), 672–682.

Heiskanen, J. (2006a). Estimating aboveground tree biomass and leaf area index in a mountain birch forest using ASTER satellite data. *International Journal of Remote Sensing* 27(6), 1135–1158.

Heiskanen, J. (2006b). Tree cover and height estimation in the Fennoscandian tundra-taiga transition zone using multiangular MISR data. *Remote Sensing of Environment* 103(1), 97–114.

Heiskanen, J. & Kivinen, S. (2008). Assessment of multispectral, -temporal and -angular MODIS data for tree cover mapping in the tundra–taiga transition zone. *Remote Sensing of Environment* 112(5), 2367–2380.

Heiskanen, J., Nilsson, B., Mäki, A.-H., Allard, A., Moen, J., Holm, S., Sundquist, S. & Olsson, H. (2008). *Aerial photo interpretation for change detection of treeline ecotones in the Swedish mountains*. Swedish University of Agricultural Sciences, Department of forest resource managemenat and geomatics, Working report 242.

Hellesen, T. & Matikainen, L. (2013). An object-based approach for mapping shrub and tree cover on grassland habitats by use of LiDAR and CIR orthoimages. *Remote Sensing* 5(2), 558–583.

Hill, R. A., Granica, K., Smith, G. M. & Schardt, M. (2007). Representation of an alpine treeline ecotone in SPOT 5 HRG data. *Remote Sensing of Environment* 110(4), 458–467.

Hofgaard, A., Løkken, J. O., Dalen, L. & Hytteborn, H. (2010). Comparing warming and grazing effects on birch growth in an alpine environment – a 10-year experiment. *Plant Ecology & Diversity* 3(1), 19–27.

Hollaus, M., Wagner, W., Maier, B. & Schadauer, K. (2007). Airborne laser scanning of forest stem volume in a mountainous environment. *Sensors* 7(8), 1559–1577.

Hollaus, M., Wagner, W., Schadauer, K., Maier, B. & Gabler, K. (2009). Growing stock estimation for alpine forests in Austria: A robust lidar-based approach. *Canadian Journal of Forest Research* 39(7), 1387–1400.

Holm, S. (1977). *Transformation av en eller flera beroende variabler i regressionsanalys (in Swedish)*. Swedish University of Agricultural Sciences, Stockholm, Hugin rapport nr 7.

Holmgren, J., Nilsson, M. & Olsson, H. (2003). Simulating the effects of lidar scanning angle for estimation of mean tree height and canopy closure. *Canadian Journal of Remote Sensing* 29(5), 623–632.

Holtmeier, F.-K. & Broll, G. (2005). Sensitivity and response of northern hemisphere altitudinal and polar treelines to environmental change at landscape and local scales. *Global Ecology and Biogeography* 14(5), 395–410.

Honkavaara, E., Litkey, P. & Nurminen, K. (2013). Automatic storm damage detection in forests using high-altitude photogrammetric imagery. *Remote Sensing* 5(3), 1405–1424.

Hopkinson, C. (2007). The influence of flying altitude, beam divergence, and pulse repetition frequency on laser pulse return intensity and canopy frequency distribution. *Canadian Journal of Remote Sensing* 33(4), 312–324.

Hopkinson, C., Chasmer, L. & Hall, R. J. (2008). The uncertainty in conifer plantation growth prediction from multi-temporal lidar datasets. *Remote Sensing of Environment* 112(3), 1168–1180.

Hudak, A. T., Strand, E. K., Vierling, L. A., Byrne, J. C., Eitel, J. U. H., Martinuzzi, S. & Falkowski, M. J. (2012). Quantifying aboveground forest carbon pools and fluxes from repeat LiDAR surveys. *Remote Sensing of Environment* 123, 25–40.

Hyyppä, J., Hyyppä, H., Leckie, D., Gougeon, F., Yu, X. & Maltamo, M. (2008). Review of methods of small-footprint airborne laser scanning for extracting forest inventory data in boreal forests. *International Journal of Remote Sensing* 29(5), 1339–1366.

Hyyppä, J. & Inkinen, M. (1999). Detecting and estimating attributes for single trees using laser scanner. *The Photogrammetric Journal of Finland* 16(2), 27–42.

Hyyppä, J., Schardt, M., Haggrén, H., Koch, B., Lohr, U., H.U., S., Paananen, R., Luukkonen, H., Ziegler, M., Hyyppä, H., Pyysalo, U., Friedländer, H., Uuttera, J., Wagner, S., Inkinen, M., Wimmer, A., Kukko, A., Ahokas, E. & Karjalainen, M. (2001). HIGH-SCAN: The first European-wide attempt to derive single-tree information from laserscanner data. *The Photogrammetric Journal of Finland* 17(2), 58–68.

Hyyppä, J., Xiaowei, Y., Rönnholm, P., Kaartinen, H. & Hyyppä., H. (2003). Factors affecting object-oriented forest growth estimates obtained using laser scanning. *The photogrammetric journal of Finland* 18(2), 16–31.

Jochem, A., Hollaus, M., Rutzinger, M. & Höfle, B. (2011). Estimation of aboveground biomass in alpine forests: A semi-empirical approach considering canopy transparency derived from airborne LiDAR data. *Sensors* 11(1), 278–295.

Jonsson, B. G., Kruys, N. & Ranius, T. (2005). Ecology of species living on dead wood – lessons for dead wood management. *Silva Fennica* 39(2), 289–309.

Jordan, G. J., Ducey, M. J. & Gove, J. H. (2004). Comparing line-intersect, fixed-area, and point relascope sampling for dead and downed coarse woody material in a managed northern hardwood forest. *Canadian Journal of Forest Research* 34, 1766–1775.

Kraus, K. & Pfeifer, N. (1998). Determination of terrain models in wooded areas with airborne laser scanner data. *ISPRS Journal of Photogrammetry and Remote Sensing* 53(4), 193–203.

Kullman, L. (1986). Recent tree-limit history of Picea abies in the southern Swedish Scandes. *Canadian Journal of Forest Research* 16, 761–771.

Kullman, L. (1998). Tree-limits and montane forests in the Swedish Scandes: Sensitive biomonitors of climate change and variability. *Ambio* 27(4), 312–321.

Kullman, L. (2010). One century of treeline change and stability - experiences from the Swedish Scandes. *The Official Journal of the International Association for Landscape Ecology, Chapter Germany (IALE-D).*

Kupfer, J. A. & Cairns, D. M. (1996). The suitability of montane ecotones as indicators of global climatic change. *Progress in Physical Geography* 20(3), 253–272.

Landsberg, J. J. & Waring, R. H. (1997). A generalised model of forest productivity using simplified concepts of radiation-use efficiency, carbon balance and partitioning. *Forest Ecology and Management* 95(3), 209–228.

Lin, Y., Hyyppä, J. & Jaakkola, A. (2011). Mini-UAV-borne LIDAR for fine-scale mapping. *IEEE Geoscience and Remote Sensing Letters* 8(3), 426–430.

Lindberg, E. (2012). *Estimation of canopy structure and individual trees from laser scanning data*. Diss. Swedish University of Agricultural Sciences. Available from: http://pub.epsilon.slu.se/8888. [Accessed 2012-11-16].

Lindberg, E., Hollaus, M., Mücke, W., Fransson, J. E. S. & Pfeifer, N. (2013). Detection of lying tree stems from airborne laser scanning data using a line template matching algorithm. In: Proceedings of ISPRS Annals – Vol. II-5/W2, Antalya, Turkey, November 11-13, 2013.

Lindgren, N. (2012). *Klassning av fjällbjörkskog enligt FAO:s definition av skogsmark med hjälp av flygburen laserskanning (in Swedish)*. Master thesis. Swedish University of Agricultural Sciences.

Lu, D., Mausel, P., Brondízio, E. & Moran, E. (2004). Change detection techniques. *International Journal of Remote Sensing* 25(12), 2365–2401.

Magnussen, S. & Boudewyn, P. (1998). Derivations of stand heights from airborne laser scanner data with canopy-based quantile estimators. *Canadian Journal of Forest Research* 28(7), 1016–1031.

Martikainen, P., Siitonen, J., Kaila, L., Punttila, P. & Rauh, J. (1999). Bark beetles (Coleoptera, Scolytidae) and associated beetle species in mature managed and old-growth boreal forests in southern Finland. *Forest Ecology and Management* 116(1-3), 233–245.

Mücke, W., Deák, B., Schroiff, A., Hollaus, M. & Pfeifer, N. (2013). Detection of fallen trees in forested areas using small footprint airborne laser scanning data. *Canadian Journal of Remote Sensing* 39, In press.

Næsset, E. (2002). Predicting forest stand characteristics with airborne scanning laser using a practical two-stage procedure and field data. *Remote Sensing of Environment* 80(1), 88–99.

Næsset, E. (2009a). Effects of different sensors, flying altitudes, and pulse repetition frequencies on forest canopy metrics and biophysical stand properties derived from small-footprint airborne laser data. *Remote Sensing of Environment* 113(1), 148–159.

Næsset, E. (2009b). Influence of terrain model smoothing and flight and sensor configurations on detection of small pioneer trees in the boreal-alpine transition zone utilizing height metrics derived from airborne scanning lasers. *Remote Sensing of Environment* 113(10), 2210–2223.

Næsset, E. & Bjerknes, K.-O. (2001). Estimating tree heights and number of stems in young forest stands using airborne laser scanner data. *Remote Sensing of Environment* 78(3), 328–340.

Næsset, E., Bollandsås, O. M., Gobakken, T., Gregoire, T. G. & Ståhl, G. (2013). Model-assisted estimation of change in forest biomass over an 11year period in a sample survey supported by airborne LiDAR: A case study with post-stratification to provide "activity data." *Remote Sensing of Environment* 128, 299–314.

Næsset, E. & Gobakken, T. (2005). Estimating forest growth using canopy metrics derived from airborne laser scanner data. *Remote Sensing of Environment* 96(3-4), 453–465.

Næsset, E. & Gobakken, T. (2008). Estimation of above- and below-ground biomass across regions of the boreal forest zone using airborne laser. *Remote Sensing of Environment* 112(6), 3079–3090.

Næsset, E., Gobakken, T., Holmgren, J., Hyyppä, H., Hyyppä, J., Maltamo, M., Nilsson, M., Olsson, H., Persson, A. & Söderman, U. (2004). Laser scanning of forest resources: The Nordic experience. *Scandinavian Journal of Forest Research* 19(6), 482–499.

Næsset, E. & Nelson, R. (2007). Using airborne laser scanning to monitor tree migration in the boreal-alpine transition zone. *Remote Sensing of Environment* 110(3), 357–369.

Nilsson, M. (1996). Estimation of tree heights and stand volume using an airborne lidar system. *Remote Sensing of Environment* 56(1), 1-7.

Nyström, M., Holmgren, J. & Olsson, H. (2012). Prediction of tree biomass in the forest–tundra ecotone using airborne laser scanning. *Remote Sensing of Environment* 123(0), 271–279.

Nyström, M., Holmgren, J. & Olsson, H. (2013). Change detection of mountain birch using multi-temporal ALS point clouds. *Remote Sensing Letters* 4(2), 190–199.

Olofsson, J., Oksanen, L., Callaghan, T., Hulme, P. E., Oksanen, T. & Suominen, O. (2009). Herbivores inhibit climate-driven shrub expansion on the tundra. *Global Change Biology* 15(11), 2681–2693.

Olofsson, K., Lindberg, E. & Holmgren, J. (2008). A method for linking field-surveyed and aerial-detected single trees using cross correlation of position images and the optimization of weighted tree list graphs. In: Proceedings of SilviLaser 2008, Edinburgh, UK, September 17-19, 2008.

Olsson, H. (1994). *Monitoring of local reflectance changes in boreal forests using satellite data*. Diss. Swedish University of Agricultural Sciences.

Pasher, J. & King, D. J. (2009). Mapping dead wood distribution in a temperate hardwood forest using high resolution airborne imagery. *Forest Ecology and Management* 258(7), 1536–1548.

Payette, S., Fortin, M. J. & Gamache, I. (2001). The subarctic forest-tundra: the structure of a biome in a changing climate. *Bioscience* 51(9), 709–718.

Persson, Å., Holmgren, J. & Söderman, U. (2002). Detecting and measuring individual trees using an airborne laser scanner. *Photogrammetric Engineering & Remote Sensing* 68(9), 925–932.

Pesonen, A., Maltamo, M., Eerikäinen, K. & Packalèn, P. (2008). Airborne laser scanning-based prediction of coarse woody debris volumes in a conservation area. *Forest Ecology and Management* 255, 3288–3296.

Pfeifer, N., Gorte, B. & Elberink, S. O. (2004). Influences of vegetation on laser altimetry – analysis and correction approaches. In: Proceedings of ISPRS Archives – Vol. XXXVI-8/W2, Freiburg, Germany, October 3-6, 2004.

Post, E. & Pedersen, C. (2008). Opposing plant community responses to warming with and without herbivores. *Proceedings of the National Academy of Sciences of the United States of America* 105(34), 12353–8.

R Development Core Team (2010). *R: A language and environment for statistical computing*. Available from: http://www.r-project.org/.

Ranson, K. J., Sun, G., Kharuk, V. I. & Kovacs, K. (2004). Assessing tundra-taiga boundary with multi-sensor satellite data. *Remote Sensing of Environment* 93(3), 283–295.

Rees, W. G. (2007). Characterisation of Arctic treelines by LiDAR and multispectral imagery. *Polar Record* 43(227), 345–352.

Reese, H. (2011). *Classification of Sweden's forest and alpine vegetation using optical satellite and inventory data*. Diss. Swedish University of Agricultural Sciences. Available from: http://pub.epsilon.slu.se/8349/. [Accessed 2012-11-16].

Rosette, J., Field, C., Nelson, R., DeCola, P. & Cook, B. (2011). A new photon-counting lidar system for vegetation analysis. In: Proceedings of SilviLaser 2011, Hobart, Australia, October 16-19, 2011.

Rouse, J. W., Haas, R. H., Schnell, J. A. & Deering, D. W. (1973). Monitoring vegetation systems in the Great Plains with ERTS. In: Proceedings of 3rd ERTS Symposium, NASA SP-351 I.

Rundqvist, S., Hedenås, H., Sandström, A., Emanuelsson, U., Eriksson, H., Jonasson, C. & Callaghan, T. V. (2011). Tree and shrub expansion over the past 34 years at the tree-line near Abisko, Sweden. *Ambio* 40(6), 683–692.

Rutzinger, M., Höfle, B., Vetter, M. & Pfeifer, N. (2011). Digital terrain models from airborne laser scanning for the automatic extraction of natural and anthropogenic linear structures. *Developments in Earth Surface Processes* 15, 475–488.

Shan, J. & Toth, C. K. (2009). *Topographic laser ranging and scanning: Principles and processing*. p 590 CRC Press.

Soininen, A. (2012). TerraScan user's guide. *TerraSolid Ltd.* Available from: http://www.terrasolid.com/download/tscan.pdf. [Accessed 2012-11-08].

Solberg, S., Næsset, E., Hanssen, K. H. & Christiansen, E. (2006). Mapping defoliation during a severe insect attack on Scots pine using airborne laser scanning. *Remote Sensing of Environment* 102(3–4), 364–376.

St-Onge, B. & Vepakomma, U. (2004). Assessing forest gap dynamics and growth using multi-temporal laser-scanner data. In: Proceedings of ISPRS Archives – Vol. XXXVI-8/W2, Freiburg, Germany, October 3-6, 2004.

Stumberg, N., Ørka, H. O., Bollandsås, O. M., Gobakken, T. & Næsset, E. (2012). Classifying tree and nontree echoes from airborne laser scanning in the forest–tundra ecotone. *Canadian Journal of Remote Sensing* 38(6), 655–666.

Ståhl, G. (1997). Transect relascope sampling for assessing coarse woody debris: The case of a $\pi/2$ relascope angle. *Scandinavian Journal of Forest Research* 12(4), 375–381.

Ståhl, G., Gove, J. H., Williams, M. S. & Ducey, M. J. (2010). Critical length sampling: a method to estimate the volume of downed coarse woody debris. *European Journal of Forest Research* 129(6), 993–1000.

Swain, P. H. & Davis, S. M. (1978). *Remote sensing: The quantitative approach*. p 396 McGraw-Hill International Book Company.

Thieme, N., Bollandsås, O. M., Gobakken, T. & Næsset, E. (2011). Detection of small single trees in the forest–tundra ecotone using height values from airborne laser scanning. *Canadian Journal of Remote Sensing* 37(3), 264–274.

Tokola, T., Löfman, S. & Erkkilä, A. (1999). Relative calibration of multitemporal Landsat data for forest cover change detection. *Remote Sensing of Environment* 68(1), 1–11.

Tømmervik, H., Johansen, B., Riseth, J. Å. A., Karlsen, S. R. R., Solberg, B., Høgda, K. a. & Hogda, K. A. (2009). Above ground biomass changes in the mountain birch forests and mountain heaths of Finnmarksvidda, northern Norway, in the period 1957-2006. *Forest Ecology and Management* 257(1), 244–257.

Ulander, L. M. H., Smith, G., Eriksson, L., Folkesson, K., Fransson, J. E. S., Gustavsson, A., Hallberg, B., Joyce, S., Magnusson, M., Olsson, H., Persson, Å. & Walter, F. (2005). Mapping of wind-thrown forests in southern Sweden using space- and airborne SAR. In: Proceedings of IGARS 2005, Seoul, Korea.

Wallace, L., Lucieer, A., Watson, C. & Turner, D. (2012). Development of a UAV-LiDAR System with Application to Forest Inventory. *Remote Sensing* 4(6), 1519–1543.

Warren, W. G. & Olsen, P. F. (1964). A line intersect technique for assessing logging waste. *Forest Science* 10, 267–276.

Waser, L. T., Baltsavias, E., Ecker, K., Eisenbeiss, H., Feldmeyer-Christe, E., Ginzler, C., Küchler, M. & Zhang, L. (2008a). Assessing changes of forest area and shrub encroachment in a mire ecosystem using digital surface models and CIR aerial images. *Remote Sensing of Environment* 112(5), 1956–1968.

Waser, L. T., Baltsavias, E., Ecker, K., Eisenbeiss, H., Ginzler, C., Küchler, M., Thee, P. & Zhang, L. (2008b). High-resolution digital surface models (DSMs) for modelling fractional shrub/tree cover in a mire environment. *International Journal of Remote Sensing* 29(5), 1261–1276.

Vastaranta, M., Korpela, I., Uotila, A., Hovi, A. & Holopainen, M. (2012). Mapping of snow-damaged trees based on bitemporal airborne LiDAR data. *European Journal of Forest Research* 131(4), 1217–1228.

Vauhkonen, J., Tokola, T., Maltamo, M. & Packalen, P. (2008). Effects of pulse density on predicting characteristics of individual trees of Scandinavian commercial species using alpha shape metrics based on airborne laser scanning data. *Canadian Journal of Remote Sensing* 34, S441–S459.

Vehmas, M., Packalén, P., Maltamo, M. & Eerikäinen, K. (2011). Using airborne laser scanning data for detecting canopy gaps and their understory type in mature boreal forest. *Annals of Forest Science* 68(4), 825–835.

Weisberg, S. (1985). *Applied Linear Regression, 2nd edition*. p 344 John Wiley & Sons, New York.

Weiss, D. J. & Walsh, S. J. (2009). Remote sensing of mountain environments. *Geography Compass* 3(1), 1–21.

Vepakomma, U., St-Onge, B. & Kneeshaw, D. (2008). Spatially explicit characterization of boreal forest gap dynamics using multi-temporal lidar data. *Remote Sensing of Environment* 112(5), 2326–2340.

White, J., Wulder, M., Vastaranta, M., Coops, N., Pitt, D. & Woods, M. (2013). The utility of image-based point clouds for forest inventory: A comparison with airborne laser scanning. *Forests* 4(3), 518–536.

Wilson, E. H. & Sader, S. A. (2002). Detection of forest harvest type using multiple dates of Landsat TM imagery. *Remote Sensing of Environment* 80(3), 385–396.

Yang, X. & Lo, C. P. (2000). Relative radiometric normalization performance for change detection from multi-date satellite images. *Photogrammetric Engineering & Remote Sensing* 66(8), 967–980.

Yu, X., Hyyppä, J., Holopainen, M. & Vastaranta, M. (2010). Comparison of area-based and individual tree-based methods for predicting plot-level forest attributes. *Remote Sensing* 2(6), 1481–1495.

Yu, X., Hyyppä, J., Kaartinen, H., Hyyppä, H., Maltamo, M. & Rönnholm, P. (2005). Measuring the growth of individual trees using multi-temporal airborne laser scanning point clouds. In: Proceedings of ISPRS Archives – Vol. XXXVI-3/W19, Enschede, the Netherlands, September 12-14, 2005.

Yu, X., Hyyppä, J., Kaartinen, H., Maltamo, M. & Hyyppä, H. (2008). Obtaining plotwise mean height and volume growth in boreal forests using multi-temporal laser surveys and various change detection techniques. *International Journal of Remote Sensing* 29(5), 1367–1386.

Yu, X., Hyyppä, J., Kukko, A., Maltamo, M. & Kaartinen, H. (2006). Change detection techniques for canopy height growth measurements using airborne laser scanner data. *Photogrammetric Engineering & Remote Sensing* 72(12), 1339–1348.

Yu, X. W., Hyyppä, J., Kaartinen, H. & Maltamo, M. (2004). Automatic detection of harvested trees and determination of forest growth using airborne laser scanning. *Remote Sensing of Environment* 90(4), 451–462.

Zhang, Y. J., Xu, M., Adams, J. & Wang, X. C. (2009). Can Landsat imagery detect tree line dynamics? *International Journal of Remote Sensing* 30(5), 1327–1340.

Ziegler, M., Konrad, H., Hofrichter, J., Wimmer, A., Ruppert, G. S., Schardt, M. & Hyyppä, J. (2000). Assessment of forest attributes and single-tree segmentation by means of laser scanning. In: Proceedings of SPIE 4035, Laser Radar Technology and Applications V, Orlando, USA, April 24, 2000.

Ørka, H. O., Wulder, M. A., Gobakken, T. & Næsset, E. (2012). Subalpine zone delineation using LiDAR and Landsat imagery. *Remote Sensing of Environment* 119(0), 11–20.

Acknowledgements

How did all this start? In the summer of 2007 I decided together with my friend from childhood, Henrik Persson, to go kayaking in the High Coast area (Sweden). We didn't want to go alone so we invited the members of the canoe club in Umeå. Eva Lindberg joined for the kayaking trip that weekend and this was the first time I heard about laser scanning and that it could be used for forestry! I got really interested and asked many questions about her PhD work, but she had not started yet… However, we kept the contact and in the winter of 2009 there was an announcement about a PhD position in laser scanning. I almost thought they had written the announcement for me as the projects included field work in the Swedish mountains! It was like a dream come true to combine challenging indoor work with lovely nature. Thank you Eva for persuading me to apply for the PhD position when we met at Uniaden in the end of January 2009.

When I started at the section in May 2009, this was a new world for me… to work with forest… I had only been running and biking in the forest, never measured the trees, not even counted them. The first thing I had to do was to plan field work to be conducted in August that summer. I'm very grateful to all the help from Riksskogstaxeringen (the Swedish National Forest Inventory) for the easy way of borrowing the equipment I needed. Thank you Anders Pålsson! Many thanks to Eva Lindberg, Håkan Olsson and Johan Holmgren for teaching me quick how to measure the forest with new high technology equipment. I was in Abisko for six weeks doing field work and I really appreciate that my main supervisor, Håkan Olsson, joined me in field the first two days to give me a flying start. I'm also very grateful for all the help from the personnel at the Scientific research station in Abisko for letting me borrow the brand new RTK-GPS and for the hospitality at the station. Many thanks to Frederic Nicholas for helping me with the field work. I have some good memories from our long

days in field and rescuing you in the snow storm. I really enjoyed the time in Abisko!

The next summer it was Abisko work again. This time to change the nature by cutting down a few trees in small patches in the forest-tundra ecotone. The forestry student Axel Bergsten helped Eva the previous year and I heard that he did a good job. I called Axel, who I just met once before and asked if he was interested in working three weeks in Abisko in June. He said yes, but probably he didn't know that we would work 12 hours a day… I also asked Thomas Johansson who I had known for some years, if he could help and he also said yes. So now we had a strong team that I knew could collect a lot of field data in the limited time I had planned. We had a really good time together, both during work and in our free time. I will never forget when we bought dishwashing gloves to paddle on inflatable mattresses in the icy water of Torneträsk and when we ran up to Abiskojaure to paddle back the 25 km on the mattresses… Thanks for your help guys and for making the field work to a true adventure!

In the winter of 2011-2012, I visited the SilviLaser conference in Tasmania. I extended the conference and visited University of Tasmania (Arko Lucieer), Forestry Tasmania (Robert Musk), CSIRO in Melbourne (Darius Culvenor), and the Department of Environment and Resource Management (John Armston). Thanks also to everyone I met during this travel and for your hospitality. I learned a lot during those months and it gave me memories for the rest of my life.

Since 2009 I have been racing with Team Haglöfs Silva in adventure racing. I'm very grateful to Håkan, who has made it possible for me to combine my PhD work with training and racing all over the world. Thanks also to my team for the support, the laughs, the challenges, and the unforgettable adventures you have given me when training and racing.

I'm very grateful to my coworkers at the Department of Forest Resource Management for enjoyable coffee breaks and lunches and for answering all my questions. My two supervisors, Håkan Olsson and Johan Holmgren, have been a great support during my PhD work. Thanks for your encouragement and for always being there when I needed you the most. Thanks also to all my coworkers at the Forest Remote Sensing section for valuable discussions and all ideas you have given me. I'm very grateful to Heather Reese for your comments and the improvements you have suggested to my manuscripts. Peder Axensten has given me many lessons about efficient programming and valuable discussions, thank you! Many thanks to Kenneth Olofsson who shared his code and contributed with valuable discussions. Kenneth and Henrik Persson have also been pre-evaluating the thesis and the manuscripts, thank you for valuable comments and suggested improvements.

In the summer of 2011 I joined a national forest inventory team for a few days in their work. Many thanks to Johan Bergstedt for inviting me to join you these days. I learnt a lot and had a great time in the forest.

The studies in this thesis are part of the research program Environmental Mapping and Monitoring with Airborne laser and digital images (EMMA), financed by the Swedish Environmental Protection Agency. Paper II was also supported by financing from the Swedish National Space Board, thank you! The laser datasets in Abisko were acquired through cooperation with the University of Lund and the national elevation model project at Lantmäteriet (the Swedish National Land Survey). The Abisko Scientific Research Station is acknowledged for supporting the work with field data acquisition. Many thanks to Blom Geomatics for arranging the laser scannings in short notice. I am also very thankful to the Swedish Defense Research Agency (FOI) for sharing the active surface code. Thanks to Taylor & Francis and Elsevier for the permission to include paper I, II, and III in this thesis. I would also like to thank the anonymous reviewers who have given constructive comments on the published articles. Many thanks to the evaluation committee, Clas-Göran Persson, Xiaowei Yu and Ole Martin Bollandsås, for constructive comments and suggested improvements in the pre-evaluation process. Since this was written before the day of dissertation, I would like to thank the opponent, Norbert Pfeifer, on beforehand for his work.

Many thanks to my family and friends for supporting me both when life is easy and hard. Thanks to Olof Häggström for helping me get started with parallel computing, it made my calculations four times faster! Finally, thanks to my lovely fiancée Helena for always supporting me and your smiles that make me happy. I love you!